

National Report of Poland to EUREF 2019

J. Krynski

Institute of Geodesy and Cartography, 27 Modzelewskiego St., 02-679 Warsaw

E-mail: krynski@igik.edu.pl

J.B. Rogowski

Gdynia Maritime University, 81–87 Morska St., 81-225 Gdynia

E-mail: jerzyrogowski@gmail.com

1. Introduction

Since 2017 the main geodetic activities at the national level in Poland concentrated on maintenance of gravity control and geomagnetic control, continuing operational work of permanent IGS/EPN GNSS stations, GNSS data processing on the regular basis at the WUT and MUT Local Analysis Centres, activities of MUT and WUT EPN Combination Centre, activity within the EUREF-IP Project, works on GNSS for meteorology, monitoring ionosphere and ionospheric storms, improving consistency between SLR and GNSS solution, maintaining the ASG-EUPOS network in Poland, modelling precise geoid, the use of data from satellite gravity missions, monitoring gravity changes, activities in satellite laser ranging and their use, geodynamics.

2. Current status of reference frames

2.1. Horizontal and vertical

The Head Office of Geodesy and Cartography (GUGiK) was continuing a field inspection of geodetic fundamental and base control network points. It is expected to be completed by the end of 2019.

2.2. Vertical

GUGiK continued preparations for a new levelling campaign in Poland. Following the existing regulations the campaign is planned to start around 2020. Major advantages of combining levelling networks with state-of-the-art GNSS measurements and gravity field models in Poland are noted.

The PL-EVRF2007-NH is in the process of being implemented by local authorities. According to Polish regulations, the EVRF2007 solution should be implemented locally by the end of 2019, at latest.

2.3. Gravity

Research activities concerning gravity field modelling and gravimetric works performed in Poland in 2018 focused on geoid modelling, evaluation of global geopotential models, determination of temporal variations of the gravity field with the use of data from satellite gravity space missions, absolute gravity surveys for the

maintenance and modernization of the gravity control, analysis of records of the superconducting gravimeter at the Borowa Gora Geodetic-Geophysical Observatory (BG) of the Institute of Geodesy and Cartography (IGiK), metrological aspects in gravimetry, and investigations of the non-tidal gravity changes.

Maintenance of gravity control and gravity survey for geodynamic research

Absolute gravity measurements were carried out on quasi-regular basis with the use of the FG5-230 gravimeter in the Jozefoslaw Astrogeodetic Observatory (JO) of the Warsaw University of Technology (WUT) since 2005 (Fig. 1). The break in repeated gravity survey between January and June 2018 resulted from the standard service of the gravimeter. Ground water level was recorded by hydrostatic piezometer and five soil moisture sensors from 0.5 m to 6.0 m depth (Krynski and Rogowski, 2018).

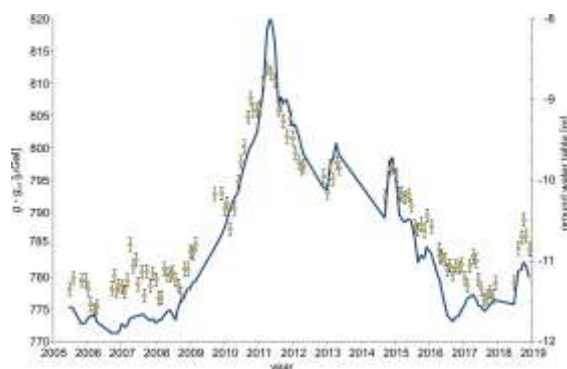


Fig. 1. Absolute gravity surveyed with the FG5-230 at Jozefoslaw (100 cm height) ($g_{ref} = 981213000 \mu\text{Gal}$)

Gravimetric investigations at BG were continued. A series of absolute gravity measurements on stations of the test network in the Observatory, conducted on monthly basis with the A10-020 gravimeter since September 2008 (Fig. 2), shows high quality of A10 gravimeter results.

The results of absolute gravity survey in Sweden with the A10-020 gravimeter in 2011–2015 were used in the definition of the new gravity reference frame of Sweden – RG 2000 (Engfeldt et al., 2018a, 2018b).

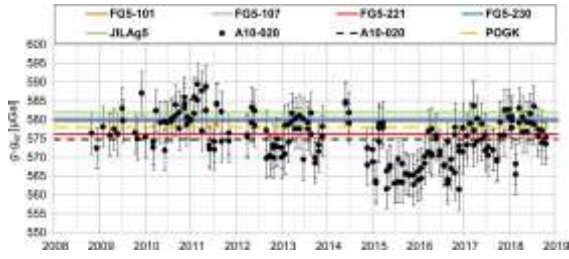


Fig. 2. Absolute gravity surveyed with the A10-020 at A-BG station in Borowa Gora (pillar level) ($g_{ref} = 981250000 \mu\text{Gal}$)

Starting from late 2014, regular measurements with the A10-020 gravimeter at three sites in BG are supplemented with the monitoring of local hydrological conditions via automated stations measuring precipitation, soil humidity (at two depths 0.1 m and 0.5 m) and water table level variation. Local hydrological model was developed (Dykowski et al., 2018a). Sensitivity of the A10 absolute gravimeter to the variation of local hydrological conditions allowing to detect small local hydrological changes was demonstrated (Fig. 3). It has also been proven that MERRA hydrological model is efficient for hydrological variations analysis.

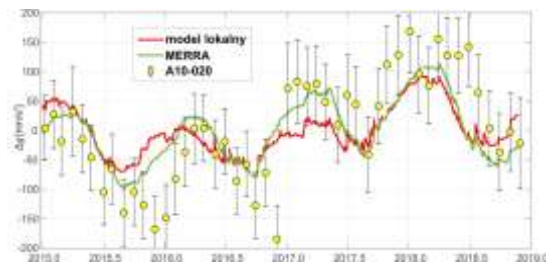


Fig. 3. Absolute gravity variations from the survey with the A10-020 at the field station 156 at BG and from local as well as MERRA hydrological models

The drift of the iGrav-027 was determined by comparison of its record with the with gravity determinations using the A10-020 absolute gravimeter at the site collocated with that of the superconducting gravimeter (Dykowski et al., 2018b). Differences obtained with fitted exponential functions are shown in Figure 4 (Dykowski et al., 2018c).

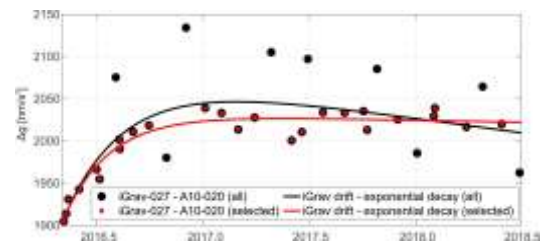


Fig. 4. Differences between the records of the iGrav-027 superconducting gravimeter and gravity determined with the A10-020 absolute gravimeter together with fitted exponential functions

The calibration of the iGrav-027 sensor was carried out during the last 70 days of 2018 with the use of two LCR G gravimeters at BG (Fig. 5).

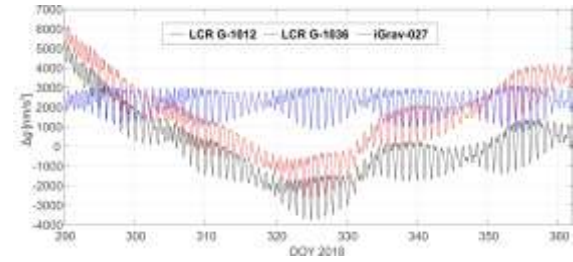


Fig. 5. Records of two relative gravimeters LCR and the iGrav-027 gravimeter

The scale coefficient for the iGrav-027 superconducting gravimeter was determined using least squares adjustment as well as Fourier transform using the amplitudes of O1, K1, and M2 tidal waves with the uncertainty of 0.4%.

In 2018, tidal data recorded in BG (iGrav-027, LCR G-1036), and in JO (ET-026) were pre-processed and submitted to the International Geodynamics and Earth Tide Service (IGETS) (Krynski et al., 2019b), (Kuczynska et al., 2018b).

The A10-020 gravimeter has been successfully used to complete the first stage of the establishment of the gravity control in Ireland island (Fig. 6). In 2018 both gravity and the vertical gravity gradient were determined at 27 of 67 gravity control stations (Krynski et al., 2019a, 2019b).

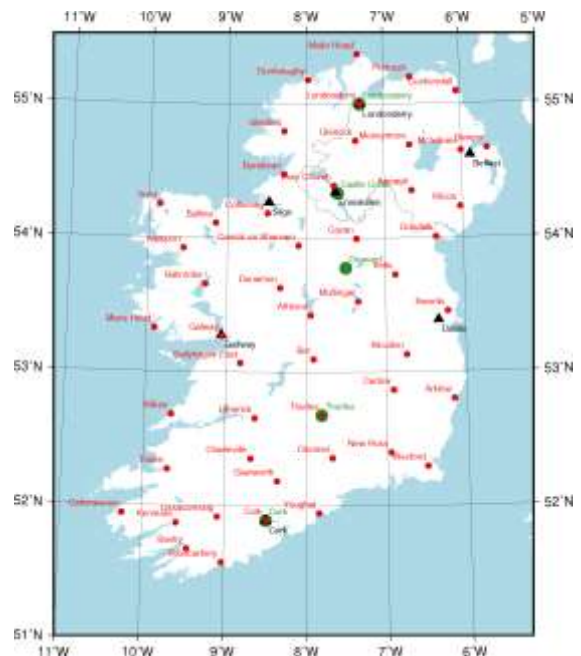


Fig. 6. Gravity control in Ireland island

In addition 8 gravimetric control points in Denmark were re-surveyed with the A10-020 gravimeter (Fig. 7) (Krynski et al., 2019a, 2019b).

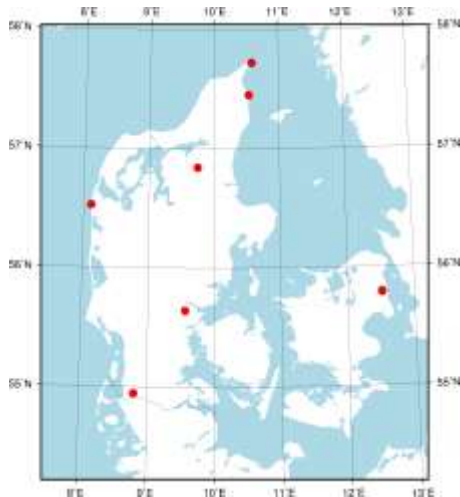


Fig. 7. Gravity control stations in Denmark re-surveyed in 2018 using the A10-020 gravimeter

Changes of gravity at the stations of the national gravity control in Poland were discussed (Barlik et al, 2018). In the southern region of Poland strong correlation of gravity changes with global hydrology was observed while stronger correlation with local hydrological environment influence was observed in the central and northern Poland. Biggest gravity changes noted at Wroclaw and Bialowieza stations are associated with reconstruction of the neighbourhood of the station (Krynski et al., 2019b).

2.4. Magnetic

Magnetic control in Poland, consisting of 19 magnetic repeat stations maintained by IGiK is supported by two magnetic observatories run by the Institute of Geophysics of the Polish Academy of Sciences (IGF PAS): Central Geophysical Observatory in Belsk and Magnetic Observatory in Hel. In addition, there are two permanent magnetic stations: Borowa Gora – run by IGiK, and Suwalki – run by IGF PAS



Fig. 8. Magnetic stations surveyed in 2018 (red dots) and magnetic observatories

Measurements of three independent components of the magnetic intensity vector, i.e. declination (D), inclination (I) and the module of the magnetic intensity vector (F) were performed in 2018 at 5 repeat stations of the fundamental magnetic control (Fig. 8).

3. Participation in IGS/EPN permanent GNSS networks

3.1. Operational work of permanent IGS/EPN stations

Permanent IGS and EPN GNSS stations operate in Poland since 1993. Recently 19 permanent GNSS stations (Table 1) operate in Poland within the EUREF program (BOGE station at Borowa Gora Observatory operates as the EPN station since 5 May 2019) of which 6 operate also within the IGS network¹ (Fig. 9). Data from those stations are transferred via internet to the Local Data Bank for Central Europe at Vienna, Austria as well as to the Regional Data Bank at Frankfurt/Main, Germany. Together with data from other corresponding stations in Europe, they were the basis of the products that are applied for both research and practical use in geodesy, surveying, precise navigation, environmental projects, etc.

Four of those stations, i.e. BOGI, BOR1, JOZ2 and WROC participated also in IGS Real-time GNSS Data project. Two stations WROC and BOR1 are also included into the IGS Multi-GNSS Experiment (MGEX) pilot project².

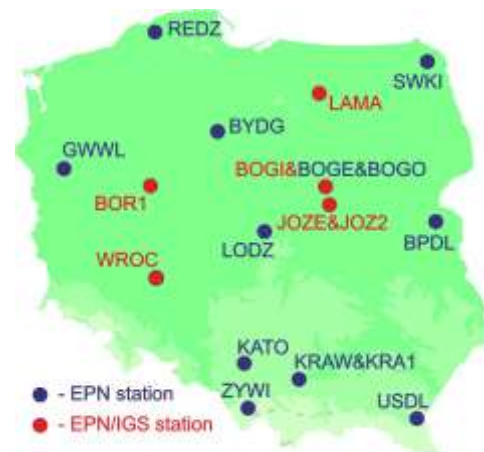


Fig. 9. EPN/IGS permanent GNSS stations in Poland (2018)

The EPN stations at Borowa Gora (BOGI), Borowiec (BOR1), Jozefoslaw (JOZ2, JOZ3), Cracow (KRAW, KRA1), Lamkowko (LAM5), and Wroclaw (WROC) take part in the EUREF-IP project³ (Fig. 10).

¹ http://www.epncb.oma.be/_networkdata/stationlist.php

² <http://igs.org/mgex>

³ http://igs.bkg.bund.de/root_ftp/NTRIP/streams/streamlist_euref-ip.htm

Since March 2005 Ntrip Broadcaster is installed at the AGH University of Science and Technology⁴. The Ntrip Caster broadcasts RTCM and raw GNSS data from KRAW0 and KRA10 sources take part in the EUREF-IP project and provide data to regional EUREF broadcasters at BKG, ASI and ROB.



Fig. 10. Polish EPN stations participating in the EUREF-IP project (2018)

Table 1. Permanent GNSS stations in Poland (2018)

Name (abbreviation)	Latitude	Longitude	Status
Biała Podlaska (BPDL)	52°02'07"	23°07'38"	EPN
Borowa Gora (BOGE)	52°28'31"	21°02'06"	EPN
Borowa Gora (BOGI)	52°28'30"	21°02'07"	IGS/EPN
Borowa Gora (BOGO)	52°28'33"	21°02'07"	EPN
Borowiec (BOR1)	52°16'37"	17°04'24"	IGS/EPN
Bydgoszcz (BYDG)	53°08'04"	17°59'37"	EPN
Gorzow Wielk. (GWWL)	52°44'17"	15°12'19"	EPN
Jozefoslaw (JOZE)	52°05'50"	21°01'54"	IGS/EPN
Jozefoslaw (JOZ2)	52°05'52"	21°01'56"	IGS/EPN
Katowice (KATO)	50°15'11"	19°02'08"	EPN
Krakow (KRAW)	50°03'58"	19°55'14"	EPN
Krakow (KRA1)	50°03'58"	19°55'14"	EPN
Lamkowko (LAMA)	53°53'33"	20°40'12"	IGS/EPN
Lodz (LODZ)	51°46'43"	19°27'34"	EPN
Redzikowo (REDZ)	54°28'21"	17°07'03"	EPN
Suwalki (SWKI)	54°05'55"	22°55'42"	EPN
Ustrzyki Dolne (USDL)	49°25'58"	22°35'09"	EPN
Wroclaw (WROC)	51°06'47"	17°03'43"	IGS/EPN
Zywiec (ZYWI)	49°41'12"	19°12'21"	EPN

⁴ <http://home.agh.edu.pl/~kraw/ntrip.php>

3.2. GNSS data processing at WUT LAC

The WUT operates the WUT EPN Local Analysis Centre (LAC) since 1996. WUT AC contributes to EUREF with final (weekly and daily) and rapid daily solutions of the EPN subnetwork. At the end of 2018, the WUT LAC subnetwork (Fig. 11) consisted of 128 GNSS stations (11 new stations were added in 2018) from which 94% observed both GPS and GLONASS satellites and 54% observed also Galileo satellites.

GNSS data are processed in WUT LAC using the Bernese GNSS Software v.5.2. Since 2010, WUT operational solutions were based on GPS and GLONASS observations. In 2018, WUT started generating 3GNSS test solutions (GPS, GLONASS, Galileo). These solutions were provided to the EPN Combination Centre to analyze the impact of adding Galileo observations on EPN combined coordinates.

In 2018, WUT AC started creating new solutions, in which the WUT regional subnetwork was augmented by global IGS reference stations. The purpose of creating those solutions is to analyze the impact of adding global stations on station coordinates of the regional network.

WUT products, i.e., daily and weekly coordinates in SINEX format and zenith tropospheric delays, can be accessed from EPN data centers: BKG⁵ and EPN⁶.



Fig. 11. EPN stations providing data processed at WUT EUREF LAC (10 April 2019)⁷

3.3. Data processing at MUT LAC

The Military University of Technology in Warsaw (MUT) LAC Analysis Centre provides final (daily and weekly) and rapid solutions processing data from 145 EPN stations (Fig. 12) distributed homogeneously over Europe. Since GPS week 1999 three new EPN stations from Ukraine (KRRS, MKRS and ZPRS) were added to MUT

⁵ <ftp://igs.bkg.bund.de/EUREF/products>

⁶ <ftp.epncb.oma.be/epncb/product/clusters>

⁷ <http://www.epncb.oma.be/>

subnetwork. The GAMIT/Globk v.10.61 software is used in MUT AC to process GNSS data.



Fig. 12. EPN stations providing data processed at MUT EUREF LAC (10 April 2019)⁸

MUT processes also local GNSS data and provides the station monitoring service⁹. The latest release uses the observations from over 550 permanent stations located in Poland and neighbouring countries. Four GNSS networks: national ASG-EUPOS and three private networks VRSnet.pl, SmartNet Poland, and TPI NetPro as well as several single stations are monitored. The applied processing strategy is similar to that used by the MUT EPN AC. Long-term analyses showed an average difference in coordinates at the reference stations of 1.4 mm for horizontal components and of 2.7 mm for heights

3.4. Activities of MUT and WUT EPN Combination Centre

In 2018, the EPN Analysis Combination Centre (ACC) continued to combine GNSS coordinate solutions, provided in the SINEX format, by 16 EPN Analysis Centres into official EPN solutions.

Since the week 1980 (17–23 December 2017) the troposphere modelling was harmonized among ACs, i.e. all EPN ACs started to use the VMF1/ECMWF approach (before the week 1980, 9 ACs used VMF1/ECMWF, and 7 ACs used GMF/GPT approach). After the week 1980 better consistency between AC coordinate solutions was observed for some stations. Also, the scale differences between the combined solution and solutions provided by BKG, IGE and ROB ACs noticeably decreased (Liwosz and Araszkiwicz, 2018).

In 2018, the ACC also analyzed the impact of including Galileo observations into EPN AC products on combined EPN station positions. In the test phase (EPN LAC Mail no. 2344), seven ACs

(BEK, BKG, IGE, ROB, UPA, NKG, WUT) provided solutions including Galileo observations (in addition to operational solutions). In comparison with the operational combined solutions, mean position differences (over 33 weeks) for the majority of stations did not exceed 1 mm in the horizontal components, and 3 mm in the vertical component.

3.5. Other EPN and IGS activities

GNSS for meteorology

The accuracy and homogeneity of Zenith Total Delay (ZTD) series estimated from ground-based GNSS data strongly depends on the data processing procedure, e.g. cut-off angle, elevation-dependent data weighting, mapping function and other details of the tropospheric model. Depending on the application targets (weather forecasting vs. climate monitoring), the requirements in terms of accuracy and homogeneity might be different. The study conducted at the University of Warmia and Mazury in Olsztyn (UWM) in collaboration with the French National Geographic Institute (IGN LAREG) and ENSTA Bretagne, France, was intended to assess the impact of some not much investigated so far GNSS data processing aspects on the quality the derived ZTD series for climate applications (Stepniak et al., 2018).

Results from more than 100 permanent stations using different strategies, options and software were analysed. PPP and DD solutions were processed with Bernese GNSS Software v.5.2 using different orbit and clock products, as well as PPP solutions using GIPSY-OASIS II with integer and float ambiguities. Estimated ZTD and IWV were inter-compared and compared to ERA-Interim and ERA5 reanalysis.

The results obtained indicate that PPP solutions have more ZTD estimates and fewer outliers than DD solution, mainly because there is no impact of a gap at other stations of network. Moreover, compared to ERA-Interim/ERA5, they have smaller biases and RMS errors and also higher correlation than DD solutions (Fig. 13). Orbits and clock products have negligible impact on PPP solutions (STD ~ 1mm), the choice of mapping function has a slightly bigger impact (STD ~ 1.7 mm). Fixing phase ambiguities to integer values in PPP mode seems to have only a marginal impact on ZTD estimates, but there is a strong sub-diurnal signal (Fig. 14). However the results seem to depend on the equipment (receiver and antenna) of the stations.

⁸ <http://www.epncb.oma.be/>

⁹ http://www.gnss.wat.edu.pl/cibdg/refimon/mutr_new.html

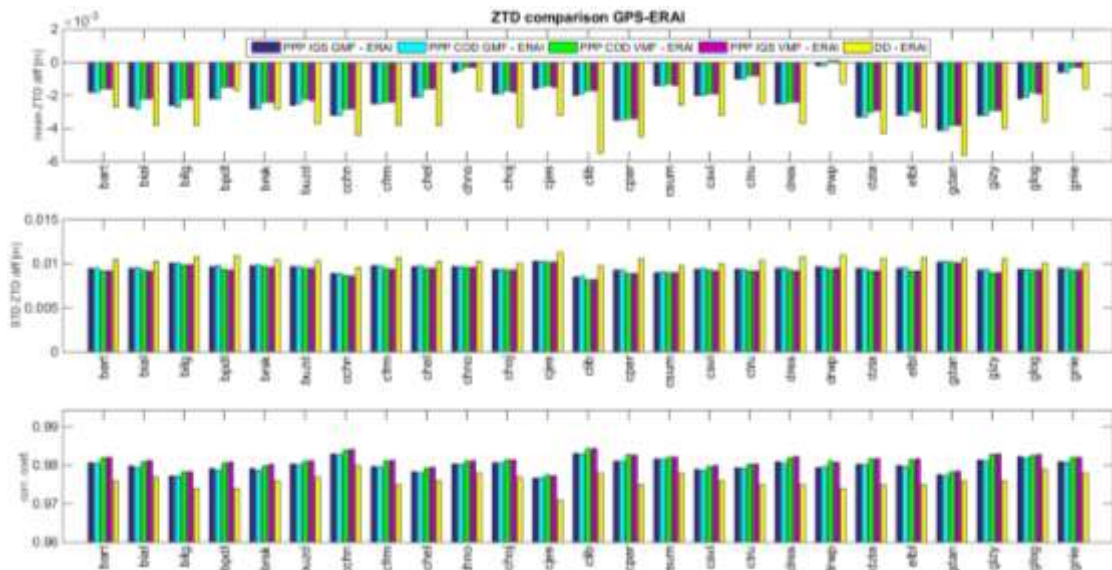


Fig. 13. Mean, standard deviation of ZTD differences and correlation coefficient between ERA-Interim and GPS solutions

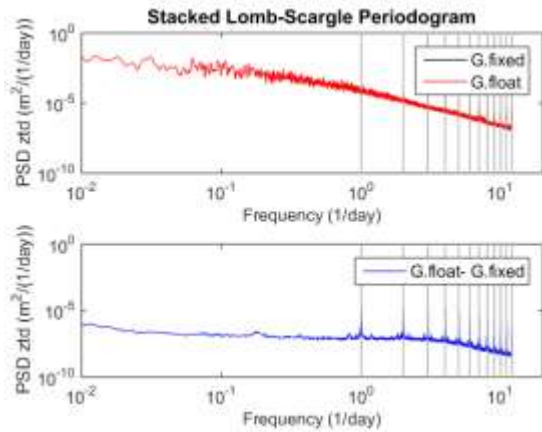


Fig. 14. Stacked Lomb-Scargle periodograms and ZTD and ZTD difference, PPP fixed and float solutions

Studies in the recent decades demonstrate the importance of remote sensing applications of the GNSS, such as in meteorology, especially in regions with low density of conventional/automatic stations and/or meteorological radars, like in Amazonia, Brazil. GNSS meteorology data constitutes this additional source of IWV estimation and is also useful in data assimilation in numerical models for weather forecasting and climate studies. The cooperation of UWM with the Shanghai Astronomical Observatory (SHAO) of the Chinese Academy of Sciences (CAS) and Federal University of Pará, Brazil, resulted in research on the assessment of GNSS IWV over central and north-eastern Amazonia (Mota et al., 2018). For that, one-year (2017-2018) of GNSS data from the Brazilian Continuous Monitoring Network (RBMC) were collected and processed (Fig. 15). GNSS data were used to estimate of ZTD and IWV with 15-min interval at each station and correlated with the

diversity and peculiarity of meteorological systems and consequent different nature and the diurnal cycle of precipitation across the Central and Northern Amazonia to the northern coast of South America. The Amazonian locations have different physiographical and meteorological characteristics, with relatively large annual rainfall accumulations, varying from about 2000 mm/year in central Amazonia to approximately 3000 mm/year on its coastal counterpart, and large amounts above 3000 mm/year in the north-western Amazonia. The diurnal cycle of rainfall, precipitation features, and the type of rainfall vary considerably in the region, where the initiation of convective squall lines in afternoon hours, parallel to the coastline, penetrate and even cross the whole basin. Those differences were assessed with the distribution of IWV at all GNSS stations. The retrieving of GNSS IWV propitiates additional indicative of water vapour convergence–advection, identification of cold pool formation and transition from shallow to deep convective systems in the region, proving that they are reliable for studies of the rainfall and convection in the tropics.

High correlation between GNSS IWV and those calculated by radiosonde was observed. The mean estimates of ZTD and IWV pattern followed the mean diurnal cycle of rainfall at all stations considered, with a well-defined diurnal cycle of these parameters at station BELE. As for the composites of ZTD and IWV based on the mean diurnal cycle of rainfall, there was a consistent behaviour in increasing ZTD and IWV four hours before the rainfall. The rate of change of these parameters two hours before the rainfall increased and occurred a diminishing of ZTD and IWV during the hour of rainfall accumulation.

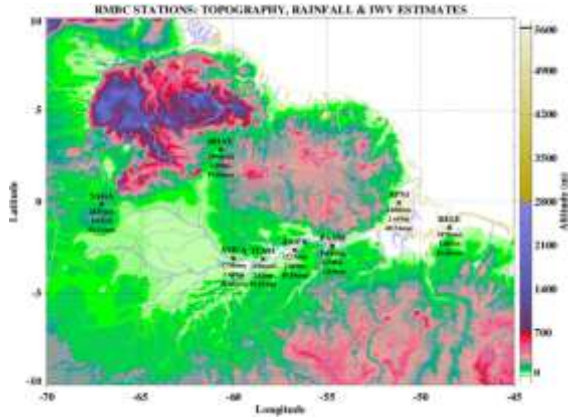


Fig. 15. Topography, mean rainfall [mm/year], mean ZTD [m], and mean IWV [mm] for the samples available from July 2017 to August 2018

Sensitivity of the Global Positioning System Radio Occultation (RO) profiles to cloud water and ice content within tropical cyclones in 2007-2010 was analysed (Lasota et al., (2018)). All gaseous parts of the atmosphere, liquid and ice water contained in the clouds were processed to obtain cloud bending angle profiles and compared to the non-cloud bending angle. The obtained differences with associated bending angle standard deviation led to the estimating cloud impact and cloud detection range. Meteorological parameters from ERA-Interim reanalysis and observations of Ice/Liquid Water Contents from CloudSat mission were used as input for simulations. The experiment is in line with previous findings showing the positive mean RO refractivity bias in cloudy conditions that exceeds 0.5% at the geometric height of around 7 km. Similar pattern, but greater and at higher altitude, is visible in the bending angle anomaly (around 1.6% at 8 km height). Although RO technique is widely considered as insensitive to clouds, results revealed that clouds influence on the bending angle is significant in 21 out of 50 (42%) investigated cases. Mean clouds' impact is detectable between 9 and 10 km, while for single observations this range usually spreads from 8 to 14 km. It is worth to notice, that cloud influence below 5 km is insignificant due to large increase of the bending angle error (Fig. 16). For most cases, the range, where clouds are detectable, is less than 3 km but for one case detection range extends for 7–8 km.

The state-of-art functional model applied for operational processing of ground-based GNSS observations to troposphere delays relies on the assumption of calm atmospheric conditions. Such claim is supported by a low sensitivity of post-fit residuals and horizontal gradients in estimated GNSS delays that both show weak dependence on GNSS processing strategies (Hordyniec et al., 2018a). However, the analysis of estimated GNSS delays in weather-specific conditions characterized

by rainfalls and clouds shows systematic effects when compared to modelled delays.

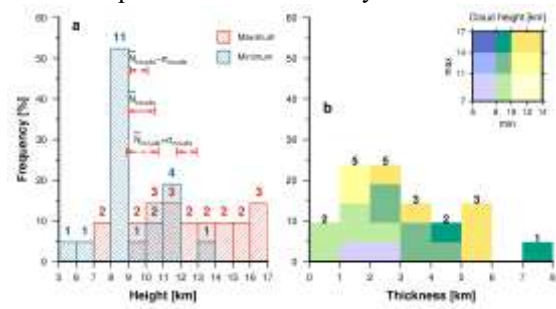


Fig. 26. Histograms for single clouds' detection ranges: (a) minimum (blue) and maximum (red) heights. Detection ranges for mean cloud contribution are presented as red horizontal arrows. (b) Thickness of detection ranges. In (b), colors indicate minimum and maximum ranges of heights where cloud's impact exceeded bending angle standard deviation. The numbers above bars indicate the number of observations

The corresponding background observation is retrieved from numerical weather prediction model using the ray-tracing technique. The path delay is a function of dry pressure, temperature and water vapour partial pressure while excluding the contribution of non-gaseous components. GNSS observations affected by precipitation or clouds, as indicated by remote sensing data and modelled ray-path trajectories, suggest a positive bias in troposphere delays with respect to results from the ray-tracing (Fig. 17). The mean differences at the level of 10-20 mm are statistically significant relative to the mean uncertainty of observations, which is at the level of 5 mm in terms of zenith delays. The approach to isolate the impact of rain and clouds on GNSS estimates requires a rigorous computation of path delays from a weather prediction model ensuring sufficiently accurate forecasts. An improvement in sensitivity of GNSS observations on particular weather conditions could be achieved by additional parameterization of the atmosphere to aid the GNSS estimation.

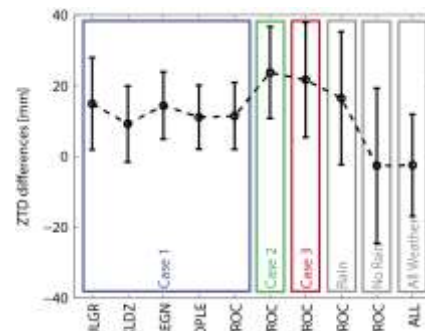


Fig. 17. Differences in ZTD from GNSS and ray-traced delays for Case 1: moderate clouds and rain; Case 2: clouds; Case 3: heavy rain and weather-specific conditions (grey panels)

The concept of GPS radio occultation (RO) soundings utilizes a receiver placed on a low Earth orbit to measure the accumulated atmospheric contribution along the limb. The estimated Doppler frequency shifts can be related to tropospheric profiles by solving the inverse problem in spherically symmetric atmosphere. The RO inversion involves transformation of the atmosphere-induced excess delay in a function of time to geophysical parameters in a function of space variable. The bending angle as a function of the asymptotic miss distance is a primary quantity for profiling the Earth's atmosphere. Conversion to commonly recognized meteorological variables of pressure and temperature is performed in the assumption of dry atmosphere and ideal gas law. A software for profiling the neutral atmosphere with RO technique has been developed at WUELS, Poland, in co-operation with NCU, Taiwan (Hordyniec et al., 2018b). The implementation of the retrieval chain for processing phase measurements from FORMOSAT-3/COSMIC mission applies the state-of-art GPS RO methodology adopted by leading processing centres. A rigorous and thorough validation were carried out to support the capability of the processing system based on independent RO retrievals and radiosonde measurements. The region within the Upper Troposphere Lower Stratosphere is particularly represented by a low uncertainty at the level of 0.5% (K) in terms of pressure and temperature differences (Fig. 18). The warm bias in the lower troposphere from comparisons of RO and radiosonde data can serve as a measure of water vapour term neglected in the retrieval.

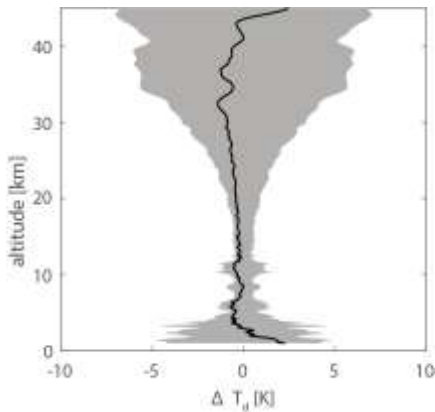


Fig. 18. Differences in the dry temperature between official and retrieved profiles in terms of mean bias (black line) and one standard deviation (grey area)

The forward modelling of RO profiles is commonly based on gaseous background fields of the refractive index. The highest contribution to profiles of the neutral atmosphere comes from the dry term and the water vapour term. In the spherically symmetric atmosphere, the refractive

index is related to the bending angle profile via the Abel transform. The extinction by particle scattering induced by the liquid and solid water in the atmosphere is neglected in comparison with background models. The yearly analysis of Global Forecast System (GFS) background fields suggests a considerable cloud fractions in all major climate zones (Hordyniec, 2018). The most statistically probable values for the liquid water content (LWC) reach 1.5 g/m³ and the ice water content (IWC) is generally within 0.3 g/m³. The fractions expressed in terms of liquid water term and ice water term in the refractivity formula correspond to 2 ppm and 0.2 ppm, respectively. Their vertical structures are usually characterized by single-spike profiles that are the most pronounced at the altitude range of 2 – 6 km for the liquid water and 10 – 12 km for the ice water. The latter one commonly referred to as the Upper Troposphere Lower Stratosphere (UTLS) is a core region for GPS RO technique in terms of particularly small retrieval uncertainty. The underestimation of background model due to neglected ice clouds can contribute to the fractional error of refractivity at the level of 0.5% in the presence of exceptionally high IWC values up to 1 g/m³. Significant contributions of the liquid water in tropical latitudes can be as large as 2% (LWC > 4 g/m³) as illustrated in Fig. 19. Simulation experiments suggest that the horizontal distribution of significant clouds should be considered in the forward modelling of RO profiles to minimize the overestimation in the assumption of spherical symmetry imposed by the Abel transform.

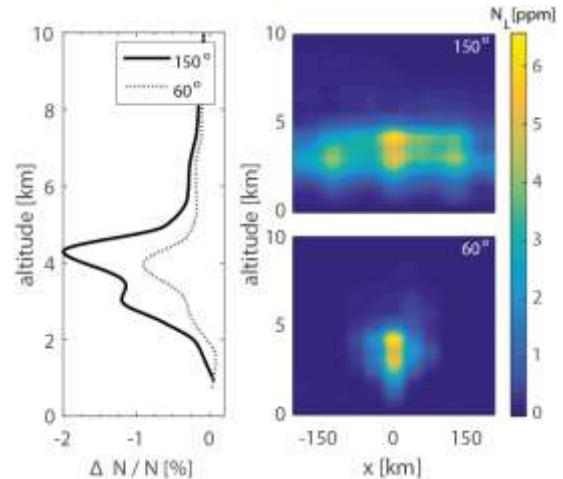


Fig. 19. Refractivity fractional errors simulated for the liquid water at different cross-sections: 60 degree (dashed grey line) and 150 degree azimuth (black solid line)

Thanks to the CNES multi-GNSS real-time corrections the users are able to take advantage of the four-system constellation in positioning. However, they have to face the real-time processing regime, thus these products may be affected by the outliers. Additionally, some problems with

availability may occur due to the numerous issues. The comprehensive analysis of availability and quality was presented (Kazmierski et al., 2018b). The orbit quality was verified in three approaches: 1) comparison with MGEX final solution, 2) analysis of the post-fit residuals when fitting continuous orbital arcs, 3) using SLR observation. Additionally, clocks stability was checked. The positioning performance for different GNSS combinations was examined. The overall availability median for all the systems reached 90% when excluding BeiDou for which some problems with data decoding occurred during the test period. The 3D orbit RMSs over a one-month test period are illustrated in Figure 20. Other validation methods confirmed, that the hierarchy of products quality is as follows: GPS, GLONASS, Galileo, and BeiDou. In the case of clocks validation, the best performance was obtained by GPS with clock standard deviation equal to about 3 cm. GLONASS and Galileo clock differences did not exceed 10 cm, while BeiDou clocks have a standard deviation of about 11 cm. Galileo and GPS IIF had the most stable clocks in a short period and the latter performed better in a longer integration time. BeiDou and GLONASS clocks stability was comparable and it was noticeably worse than for GPS and Galileo. The positioning tests indicated that additional GNSS mainly reduce formal errors due to the improved satellite geometry. However, in the case of the coordinate bias the results are comparable or even worse than those obtained for GPS-only solution.

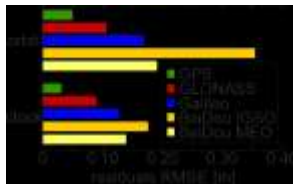


Fig. 20. RMSE of real-time orbits and clocks compared to the CODE MGEX solutions for 1–30 April 2016

Due to the fact that the quality of real-time products is not homogenous among systems, it is necessary to use appropriate observation weights in multi-GNSS processing. Therefore, several

observation weighting schemes, that are suitable for real-time multi-GNSS PPP, were developed and compared (Kazmierski et al., 2018a). In order to find the best weighting approach the following factors were taken into account: formal errors of coordinates, coordinate repeatability, and solution convergence time. Two schemes with equal weight for all systems with a different ratio between pseudorange and carrier-phase observations were tested. Also schemes that use information about observation noise, and a scheme that uses Signal in Space Range Error (SISRE) were tested. The last scenario uses both information about observation noise and SISRE parameter. Those five scenarios are presented in Figure 21.

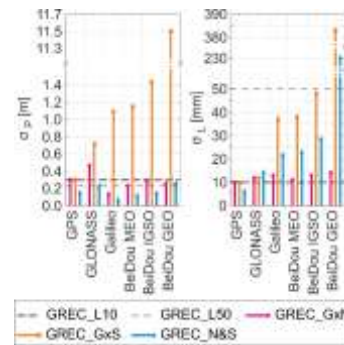


Fig. 21. Comparison of weighting schemes for (left) pseudoranges and (right) carrier-phase measurements

The best results were obtained for the weighting scheme which contains information about the quality of the products that were used in the processing. The information about the quality of products was expressed by the SISRE parameter. All the results were compared with the GPS-only solution. The coordinate repeatability was improved by 6%, an average reduction of formal errors was equal to about 38% in each coordinate component. In the case of convergence time, the improvement was equal to 47% and 39% for horizontal and vertical component, respectively (Fig. 22). Summarizing, the multi-GNSS constellation can improve the quality of the estimated coordinates and may shorten convergence time of PPP solution.

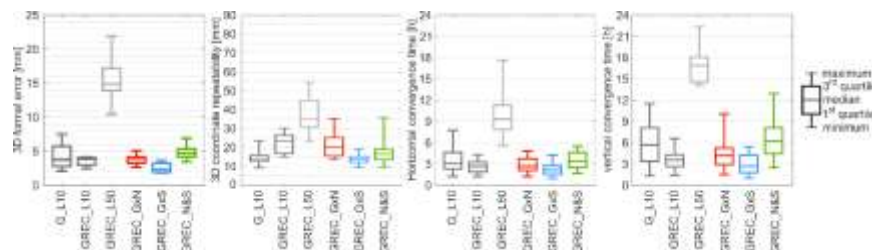


Fig. 22. From the left: 3D formal errors of coordinates, 3D coordinate repeatability, horizontal convergence time, vertical convergence time in static PPP using different weighting schemes

The kinematic experiment was performed in order to evaluate the proposed weighting scheme. The test was carried out on a 26 km long distance with varying intensity of infrastructure (Fig. 23).



Fig. 23. Number of epochs with proper solution (top), number of visible satellites (bottom)

Two weighing schemes with equal weights for all the systems with a different ratio between code and phase observations were evaluated. Additionally, a variant based on the SISRE parameter was tested as the best one during static mode positioning (Kazmierski, 2018). The use of GPS, GLONASS, Galileo, and BeiDou satellites increased the number of positioning epochs possible to be determined by 10%. This gain was especially valuable in a fast-changing environment with a substantial horizon coverage by buildings, trees, trucks etc. In the open area, all tested variants ended with comparable results. The advantage of the proposed weighting scenario was observed in the environment with a bigger number of obstacles. SISRE weighting scenario allowed the horizontal component RMS to remain below 0.2 m. The Up component quality was not as good as the horizontal one, but the proposed scenario brought the lowest RMS. The dense infrastructure decreased the position accuracy and the solution quality was about 1 m and 2 m for the horizontal and vertical component, respectively. However, this result was much better than the one obtained from the GPS-only solution for which RMS reached 4.5 m. It showed that the appropriate weighting approach may improve the RMS in the SPP solution by 13% and 42% for the horizontal and vertical coordinate components, respectively. The quality of the vertical component in the multi-GNSS PPP solution was comparable with those obtained with GPS-only. However, the improvement of the horizontal coordinate reached up to 70% when compared with GPS.

Monitoring ionosphere and ionospheric storms

In 2018, the Institute of Geodesy of UWM continues development of its regional UWM-TEC

ionosphere maps. The overall processing of producing UWM-TEC maps, proposed by IG/UWM team, is based on a three-step procedure: step 1: Estimation of the carrier phase bias; step 2: TEC calculation at the ionospheric piercing points (IPPs); step 3: TEC interpolation to form a regular grid (TEC map).

The accuracy of the resulting UWM-TEC maps depends primarily on the accuracy of the estimated carrier phase bias for each continuous data arc. Krypiak-Gregorczyk and Wielgosz (2018) proposed and validated a methodology for accurate bias estimation of the phase function LGF (geometry-free linear combination) for the use in GNSS-based regional ionospheric modelling. The accuracy of the estimated bias was determined by the analysis of its repeatability over the day-to-day boundaries for GPS and GLONASS satellites. Test results show that the bias accuracy (RMS) is at the level of 7-8 cm, i.e. below 1 TECU, depending on the selected data elevation cut-off.

The regional UWM-TEC maps are characterized by 2-minute time interval and 0.2° spacing in both latitude and longitude. The accuracy of the vertical TEC maps is assumed to be better than 1 TECU (Krypiak-Gregorczyk et al., 2017). The new highly accurate and high-resolution regional ionospheric TEC model based on multi-GNSS carrier phase data was applied for studies on the response of the ionosphere layer to the largest geomagnetic storms during Solar Cycle 24. All three storms took place near the spring equinox in the years 2012, 2013, and 2015. The quality of the highly accurate and high-resolution ionosphere model was tested by a comparison to the broadly used Global Ionosphere Maps (GIMs) provided by the IGS. In addition, critical frequency foF2 data from two ground-based ionosondes located in Europe was used for comparisons with GNSS estimates.

The analyses of the ionosphere dynamics during severe geomagnetic storms conveyed very well the nature of changes taking place in the ionosphere. It should be stressed that, as reported by Astafyeva et al. (2015), the commonly available ionospheric maps with the temporal resolution of 1-2 hours and low spatial resolution may be insufficient for a detailed analysis of momentary effects of the storm. The obtained results showed that the regional ionospheric model UWM-TEC based on phase observations provides useful information on the ionosphere's response to geomagnetic disturbances. The UWM-TEC maps ensure more complete information on the ionosphere's response to magnetic disturbances than the currently available TEC maps (Fig. 24, Krypiak-Gregorczyk, 2018).

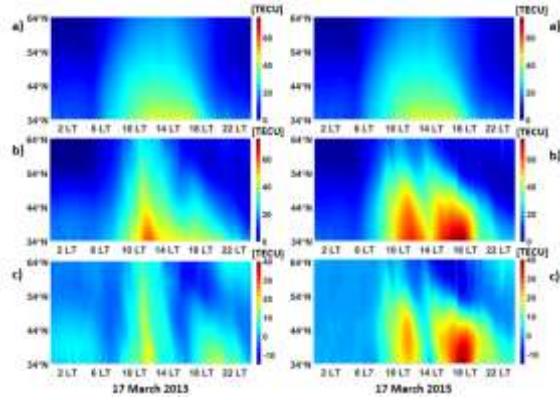


Fig. 24. Changes in the condition of the ionosphere, observed by the UWM-TEC model: (a) calm ionosphere, (b) disturbed day (17 March), (c) changes in the condition of the ionosphere in relation to the calm period for 2013 (the left panel) and 2015 (the right panel) (Krypiak-Gregorczyk, 2018)

The precise point positioning (PPP) and the least-squares collocation (LSC) modelling method are applied in the creation of regional Total Electron Content (TEC) model in Southeast Asia (Jarmolowski et al., 2018). The Leave-one-out (LOO) validation of the covariance parameters applied epoch by epoch, assured the optimal parametrization of LSC modelling. The model is based on IGS stations, which have a relatively homogeneous distribution there. The developed stochastic model (PPPLSC) is compared with the well-known stochastic global UQRG model, which is interpolated by the ordinary kriging (OK) and CODG global TEC model based on spherical harmonics (SH), and also the IGSG model, which is a combination of several models developed by the IGS Ionosphere Associate Analysis Centers. These four models derived from different approaches are assessed together using self-consistency analysis based on a geometry-free combination of carrier-phase observations, and also using external validation employing dual-frequency altimeter TEC from three low-Earth-orbit satellites: Jason-2, Jason-3 and Sentinel-3A. The self-consistency analysis of TEC models with the use of carrier-phase observations proves a better consistency of stochastic models in relation to TEC models based on SH. The set of statistical values of external comparisons with three altimetry-derived trajectories of TEC observations additionally confirms the advantage of stochastic PPPLSC and UQRG models. The validation results all together indicate a better quality of stochastic models in relation to those based on the summation of spherical functions, because the latter models lose the higher frequency signal due to the spectral limitation coming from the low order SH applied in IGSG and CODG.

The Gdansk University of Technology in collaboration with the Department of Radiophysics

of Geospace of the Institute of Radio Astronomy NAS of Ukraine in Kharkiv improved the original method for estimating TEC variations using satellites with high elevation angles (Nykiel et al., 2018). The use of signals received from two satellites allows creating separated TEC variations maps for each of them. Thereafter, they can be used for the determination of the height of the ionospheric inhomogeneities (HII) by estimation cross-correlation coefficients between the maps. In general, the proposed method allows to describe the characteristics of the ionospheric disturbances in the 4D space: latitude, longitude, altitude, and time.

The method was verified by analyzing ionospheric events before, during and after the St Patrick's Day storm in March 2013. In quiet geomagnetic conditions, the obtained HII are similar to the height of peak ionospheric electron density derived from the ionosondes what is consistent with other studies. The HII increased significantly during the active phase of the storm. Obtained results confirm that the method developed allows reliable determination of the HII. However, certain conditions concerning the satellites location on the sky and their relative position, must be met. The best results were obtained when two satellites were near the highest elevation (preferably above 75° - 80°) and the angular distance between them was about 20° - 25° .

Because only GPS satellites were used in the study, the conditions for estimating the reliable values of HII were good enough only one day. In the future works more GNSS systems will be included, which should significantly improve temporal resolution and reliability of estimated HII, especially when applying cross-system calculation

4. Improving consistency between SLR and GNSS solutions

All satellites of the new GNSS/RNSS systems, i.e. GLONASS, Galileo, BeiDou, QZSS, and IRNSS, are equipped with retroreflectors for laser ranging measurements. In the case of the GPS system, only one pair of satellites of the IIA Block was equipped with retroreflectors as a part of the NAVSTAR-SLR experiment.

In recent years, there has been a very rapid development of GNSS systems. The GLONASS system became fully operational in 2010. The full operational status of the third generation of the BeiDou system was announced in December 2018. The Galileo system achieved partial interoperability in 2015, while in February 2019, after activating Galileo satellites launched in 2018, the number of active satellites increased to 24. To meet the increasing needs of GNSS users regarding the quality and availability of satellites, both the IGS and the International Laser Ranging Service (ILRS) intensified research on the use of new systems. In

2014, the first intensive ILRS campaign dedicated to tracking GNSS satellites as part of the LARGE (LAsER Ranging to GNSS s/c Experiment) initiative was held. Most laser stations have optimized the tracking capabilities of high orbiting GNSS satellites (Bury et al., 2017) and allowed a smooth transition between tracking objects when a dozen or so objects with retroreflectors are available at the same time. The work done by ILRS and in SLR observatories led to a significant increase in the number of observations to GNSS satellites, in particular to the Galileo system.

The Galileo system consists of 4 In-Orbit-Validation (IOV) satellites, of which 3 operate today and 22 Full-Operational-Capability (FOC) satellites, of which 21 are in the operational condition. The first pair of FOC satellites (E14, E18) have been launched to abnormally highly eccentric orbits, making them not fully useful for navigational purposes, however, the satellites are operational and have full potential for geodetic and experimental purposes, including experiments related to relativistic time dilatation (Zajdel et al., 2017, 2018; Kazmierski et al., 2018; Sosnica et al., 2018a).

4.1. The Blue-Sky effect

The Blue-Sky effect is one of the effects that limits the consistency between laser techniques in satellite geodesy (SLR) and microwave techniques (GNSS, VLBI, DORIS) due to the fact that SLR observations are conducted during good weather conditions (clear sky), when the surface of the Earth is deformed by high atmospheric pressure (Atmospheric Pressure Loading, Fig. 25). The geophysical Blue-Sky effect was first estimated for all SLR laser stations performing observations to LAGEOS geodetic satellites, and more recently also for laser stations performing measurements to GNSS satellites (Bury et al., 2019). The use of SLR observations to GNSS satellites was possible thanks to intense ILRS tracking campaigns and a significant increase in laser observations to the new GNSS satellites.

4.2. Troposphere delay modelling in SLR

Another effect limiting the consistency between the SLR and GNSS solutions is the difference in the tropospheric delay modelling. The susceptibility of SLR laser measurements to tropospheric delay differs from the sensitivity of microwave observations (GNSS, VLBI, DORIS) to the tropospheric signal delay. The hydrostatic delay is similar in magnitude, as it is associated with the distribution of atmospheric pressure in both optical and microwave wavelengths. In contrast, the wet delay associated with the distribution of water vapour content in the atmosphere is about 70 times

smaller in laser observations in relation to microwaves.

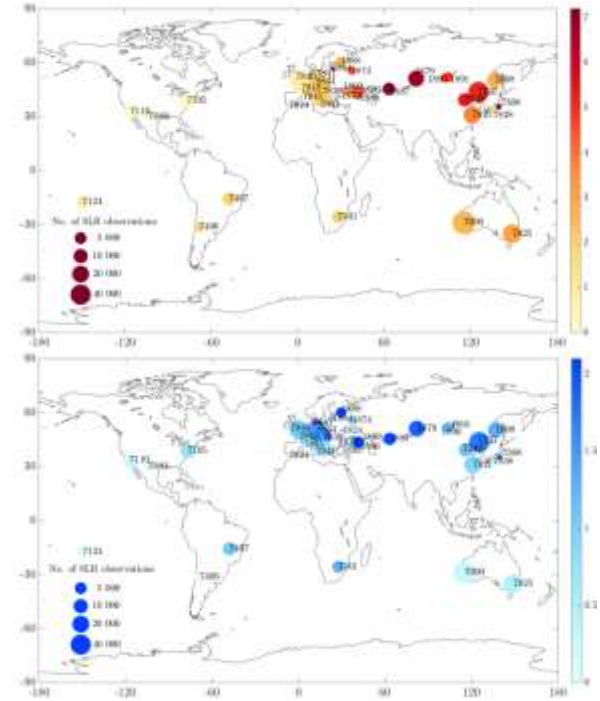


Fig. 25. Amplitude of the annual signal in the deformation of the Earth's crust caused by atmospheric pressure loading (top) and the Blue-Sky effect determined for laser stations tracking GNSS satellites (bottom); the size of the effect is denoted in color; the surface area of the symbols used is proportional to the number of SLR observations

Models of tropospheric delay dedicated to laser observations do not currently take into account horizontal gradients, which means that they assume that the atmospheric zenith (i.e. the direction of the minimal tropospheric delay) coincides with the geometric zenith (normal to the ellipsoid at a given point). The tropospheric delay function recommended by the IERS 2010 Conventions is as follows:

$$d_{\text{atm}}(e) = \mathcal{d}_{\text{atm}} \cdot m_f(e)$$

here \mathcal{d}_{atm} is the zenith delay caused by hydrostatic and wet part, and $m_f(e)$ means a common mapping function for the hydrostatic part and the wet delay at the zenith. In SLR measurements, both the zenith delay and the parameters of the mapping function are calculated on the basis of meteorological observations conducted simultaneously with laser measurements.

In order to improve modelling of the tropospheric delay in laser observations and to improve the consistency between SLR and GNSS, extending the currently used model with horizontal gradients that account for the asymmetry of the tropospheric state above laser stations was proposed:

$$d_{\text{atm}}(e) = \mathcal{E}_{\text{atm}} \cdot m_f(e) + (G_N \cos A + G_E \sin A) \cdot m_f(e)$$

Hence, the tropospheric delay in the SLR technique will be modelled in a similar way to that in the GNSS technique, taking into account the specificity of laser observations. Drozdowski and Sosnica (2018) calculated the horizontal gradients on the basis of long-term measurements to LAGEOS satellites. It turned out that SLR observations allow determining horizontal gradients

that are similar in direction and amplitude to gradients determined on the basis of hydrostatic delay from numerical weather models, while GNSS gradients are similar to the sum of hydrostatic and wet delays for most SLR-GNSS co-locations (Fig. 26).

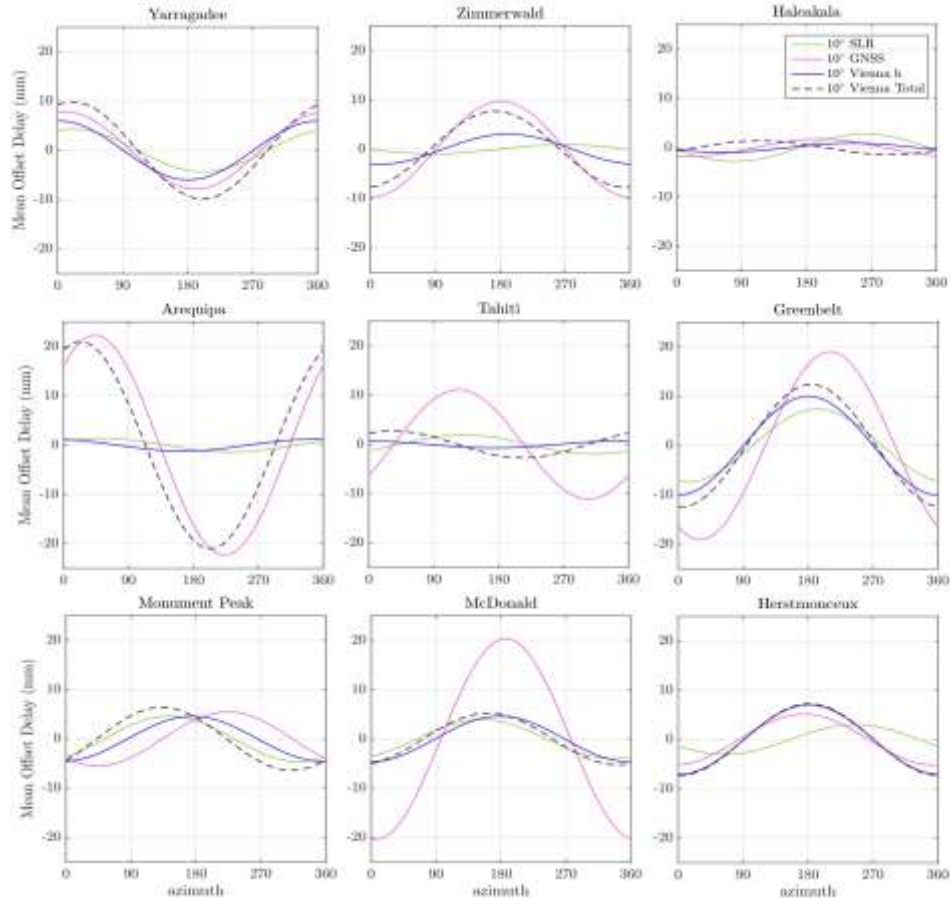


Fig. 26. Horizontal gradients of the tropospheric delay determined from SLR and GNSS observations and from hydrostatic and total tropospheric delays determined using numerical weather models (Vienna models)

4.3. Determination of global parameters using SLR tracking of GNSS

So far, the Earth rotation parameters have been determined using laser observations to geodetic satellites or microwave observations from GNSS satellites and using VLBI or DORIS observations (in a limited scope). The developed methodology of reducing systematic errors in laser observations and a significant increase in the number of SLR observations to new GNSS systems allowed the use of laser observations to GNSS satellites, which until now were not included in the determination of global geodetic parameters or realization of global geodetic reference frames.

Sosnica et al., (2018b) proposed a method of the parameter determination of SLR station coordinates, geocenter coordinates, and the Earth's rotational motion based on SLR observations to GLONASS, Galileo, BeiDou, QZSS and GPS satellites. The results obtained show that the standard SLR solutions based on LAGEOS satellites can be improved by considering GNSS observations, especially by reducing the correlation between the LAGEOS empirical orbit parameters, right ascension of the satellite ascending nodes, and the length-of-day variations (LoD). The calculated pole coordinates and LoD from the SLR technique become more consistent with GNSS microwave solutions with the reduction of the mean square

error LoD from 122.5 $\mu\text{s/d}$ to 43.0 $\mu\text{s/d}$ in the LAGEOS and LAGEOS+GNSS solutions respectively, and reduction of the mean LoD offset from -81.6 $\mu\text{s/d}$ to 0.5 $\mu\text{s/d}$ when compared to the IERS-14-C04 series, which is based on four space geodesy techniques. Thus, it was proved that the integration of two satellite geodesy techniques onboard GNSS satellites is possible with the accuracy of single millimetres.

4.4. SLR satellite signature effect

The satellite signature effect is one of the systematic effects in SLR tracking of GNSS satellites. It is related to the types of detectors used at laser stations and the flat arrays with retroreflectors installed onboard of GNSS satellites (Fig. 27). Two types of SLR detectors dominate: low-energy C-SPAD, i.e. compensated single-photon avalanche diodes and high-energy MCP/PMT, i.e. microchannel plates or photomultiplier tubes. Low energy detectors registering single photons map a full picture of the retroreflector because the probability of the laser pulse reflection from each corner cube is the same. Therefore, using observations based on many low-energy pulses sent to the satellite, one can obtain SLR measurements free from systematic effects related to the inclination of the reflector. In the case of high energy detectors registering many photons, photons reflected from the nearest edge of the retroreflector are recorded first. Due to the limited number of photons that can be registered, distances from SLR observations are shorter than actual distances, in particular in the case of inclined retroreflectors. This effect is called the satellite signature effect and was first identified in the publication on laser observations for GLONASS satellites, and then in an article describing laser observations for the Galileo IOV, FOC and FOC satellites in eccentric orbits (Sosnica et al., 2018a).

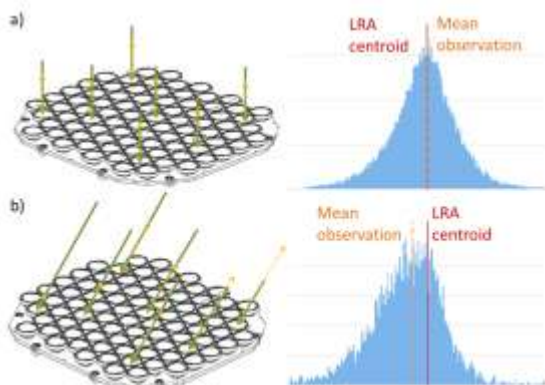


Fig. 27. Visualization of the satellite signature effect in the case of multi-photon detectors in a situation where the laser beam falls perpendicular to the retroreflector (a) and when the retroreflector is inclined in relation to the observer and the detector registers the majority of photons reflected from the nearest edge (b)

5. ASG-EUPOS network

5.1. Status of the ASG-EUPOS network

In 2018 a complex modernization of ASG-EUPOS system was carried out. Its aim was to provide real time network correction data from Galileo and BeiDou observations in addition to GPS and GLONASS.

In first stage of modernization, 58 GNSS receivers (Trimble NetR9, and Leica GR30) were upgraded. Additionally to tracking capabilities, it was intended to adjust GNSS infrastructure to multi-constellational hardware/licensing requirements of the Trimble Pivot Platform (TPP)TM software. After the upgrade, all receivers owned by GUGiK track 4 main GNSS constellations and are convergent with TPP software. Remaining GPS+GLO stations belong to foreign or external institutions (universities and research centres). Individual dialogues of GUGiK with the owners of the Polish GPS+GLO stations about possibilities of upgrading their receivers with GAL and BDS tracking capabilities are currently conducted.

The second stage of modernization, concerned an upgrade of TPP software to allow to process and store GNSS data and also to deliver both RTK and RTN corrections from 4 main GNSS constellations. The RTCM 10403.2 MSM5 format is used for real time correction streams.

At present 125 permanent reference stations are operable within the ASG-EUPOS network (86 stations owned by GUGiK are 4GNSS: GPS+GLO+GAL+BDS, 27 external stations are 4GNSS, and 1 external stations is 3GNSS and 11 stations are 2GNSS: GPS+GLO)¹⁰ (Fig. 28).



Fig. 28. Reference stations of the ASG-EUPOS system (March 2019)

¹⁰ www.asgeupos.pl

In 2019, GUGiK has planned to replace 12 GNSS antennas and upgrade an automatic post-processing software module. The antenna replacement is due to acquisition of new 4GNSS Trimble Choke Ring antennas which are going to be individually calibrated at GPS+GAL+GLO+BDS. The upgraded post-processing module is intended to be able to provide solutions on the basis of data from all four main GNSS constellations.

As the next step, reference station network is planned to be densified in the regions with the largest spacing between existing stations, which will increase availability and accuracy of real time services there. In 2018 sites for new reference stations were chosen and preliminary agreements with owners were approved.

6. Modelling precise geoid

Activities of the team of IGiK on the improvement of the accuracy of precise quasigeoid modelling for Poland were continued. The usefulness of scattered/sparse absolute gravity data, in particular dense gravity control established with the A10 gravimeter, for the validation of Global Geopotential Models (GGMs) as well as for improving geoid heights from satellite-only GGMs was demonstrated (Godah et al., 2018a).

Currently available gravity anomalies from the satellite altimetry models were compared with the shipborne and airborne gravity anomalies along the Polish coast and in the Baltic Sea and validated (Kuczynska et al., 2018a). The mean differences between the DTU10 and GMG V24.1 altimetry-derived models equal to 0.02 mGal. However, significant differences are observed in the coastal areas. Shipborne and airborne marine gravity datasets, collected over the past 65 years by various institutions, were also compared.

Furthermore, new gravimetric quasigeoid models for the territory of Poland were developed using the new gravity data from satellite altimetry, the EIGEN-6C4 GGM, and the Shuttle Radar Topography Mission (SRTM) 1 arcsec global elevation model. The accuracy of these models, estimated using data from ASG-EUPOS permanent GNSS stations, reaches 1.4 cm.

In 2020 the only vertical reference frame in Poland will be the realisation of the European Vertical Reference Frame (PL-EVRF2007-NH). Investigations concerning the definition of the new quasigeoid with the use of the existing GNSS/levelling networks (EUVN, EUVN_DA, POLREF, EUREF and ASG-EUPOS), GGMs (EGM2008, EIGEN-6C4, GECO) and the European Gravimetric Geoid Model – EGG2008 were conducted (Olszak et al., 2018). The developed models were evaluated in terms of accuracy of height anomalies. The consideration of the tidal correction to the ellipsoidal heights had the decisive

impact on the resulting models. The EVRF2007 is maintained in a zero-tide system while the ellipsoidal coordinates of stations are determined in a tide-free system. The inconsistency of these two systems, may result in the error of the height anomaly of a few centimetres. The outcome of the research provides a number of interesting conclusions concerning the competitiveness of the EGG2008 model (free from the errors of the levelling networks), especially when considering a noticeable trend of growth of residuals from the south-east to the north-west of Poland, suggesting systematic errors of the normal heights. The internal accuracy of this quasigeoid model is estimated at approx. 2.0-2.3 cm, depending on the tested group of reference points. In comparison, the best fit of the EGG2008 model to height anomalies of EUVN and ASG-EUPOS stations, evaluated at 1.3 cm, eliminates most of the systematic errors, however, is burdened with "hidden" errors related to the levelling networks.

Regional trend in the Baltic Sea level changes at eight selected tide gauge stations was determined using the available data from satellite altimetry (Lyszkowicz and Bernatowicz, 2018a). Sea level anomalies were extracted from the multi mission global product available at CMEMS and then analysed using Ferret and Hector software. They were compared with absolute mean sea level computed from tide gauge data and permanent GNSS observations was taken from the SONEL web page¹¹. Differences between the results obtained using both methods reached the level of 1 mm/year; the largest difference of 2.4 mm/year was obtained at Helsinki station. The use of longer time series, allows more reliable estimate of trend and the local sea level.

The geocentric changes of sea level at the tide gauge Wladyslawowo on the Polish coast of the Baltic Sea were presented in Lyszkowicz and Bernatowicz (2018b). They were estimated from monthly mean tide gauge records from 1951 -2017 provided by the Institute of Meteorology and Water Management and permanent and daily solutions from GNSS observations at Wladyslawowo station from April 2003 to February 2011 provided by the Nevada Geodetic Laboratory (NGL). The absolute mean sea level change at the station Władysławowo was estimated as $+2.99 \pm 0.41$ mm/year.

7. The use of data from satellite gravity missions

Quality of the newest satellite-only two GGMs: GOSG01S, Tongji-Grace02k as well as SGG-UGM-1 model combined with terrestrial data was investigated in IGiK. They were evaluated in terms of height anomalies using GNSS/levelling data at

¹¹ <http://www.sonel.org/-Sea-level-trends-.html?lang=en>

ASG-EUPOS stations. Obtained results indicate poor quality of spherical harmonics above d/o 200 in satellite-only models investigated.

The GRACE satellite mission has ended in October 2017. In 2018, the Center for Space Research at University of Texas, Austin (CSR), the GeoforschungsZentrum (GFZ) and the Jet Propulsion Laboratory (JPL) computing centers generated a new version, i.e. version 6 (Release 6 - RL06), level 2 products to improve previous solutions, i.e. version 5 (Release 5 - RL05), and to ensure compliance with GRACE Follow-On data processing standards. Using the RL06 GRACE-based GGMs generated by CSR, temporal changes of geoid heights for the area of Poland were determined. The RL06 GRACE-based GGMs used were filtered with the DDK3 filter and truncated to a degree and order of 60. The determined time series of geoid height changes for the area of Poland as well as their differences are shown in Figure 29.

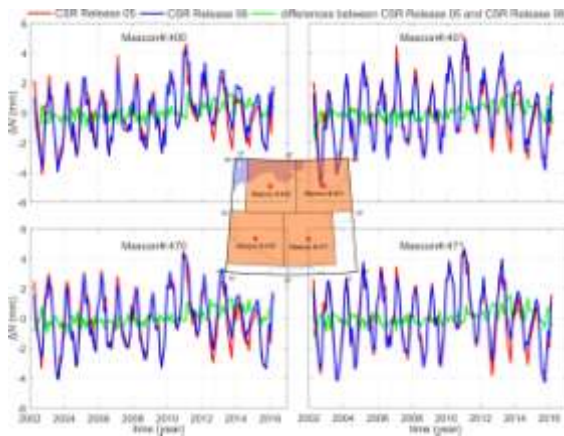


Fig. 29. Time series of geoid height variations for the area of Poland received from version 6 of GGMs developed at CSR on the basis of data from the GRACE mission

The location of the areas for which the time series of geoid height variations were determined coincides with the location of mascons which are also the products of the GRACE mission. By 2012, the differences between the temporal changes in the geoid height for the area of Poland determined on the basis of RL05 and RL06 GRACE-based GGMs developed in CSR are at the level of tenths of a millimetre. After 2012, these differences increase, reaching up to 1 mm in some cases. For this period, the application of the RL06 GRACE-based GGMs causes a noticeable change in the long-term component of time series of geoid height changes.

The suitability of data from Non-Dedicated Gravimetric Satellite Missions (NDGSM) to determine temporal changes in mass distribution in the Earth system, including temporal changes in the geoid height, and the ability to reliably supplement the time series of changes in the mass distribution during the gap between GRACE and GRACE-FO missions were investigated. The research was conducted for the territory of Poland and the Amazon basin, i.e. areas characterized by different signal strength - various temporal changes in the mass distribution.

The time series of geoid height changes obtained from GGMs developed on the basis of data from NDGSM were smoothed using a moving average with a window of three months. The results shown in Figure 30 indicate that GGMs developed on the basis of data from some NDGSM seem, to some extent, suitable for reliable determination of temporary geoid height changes for the Amazon basin. For areas with a weak signal, i.e. a small mass transport, as in the case of Poland, the GGMs developed on the basis of data from NDGSM are unsuitable for determining temporal changes in the geoid height (Godah et al., 2018c, 2019).

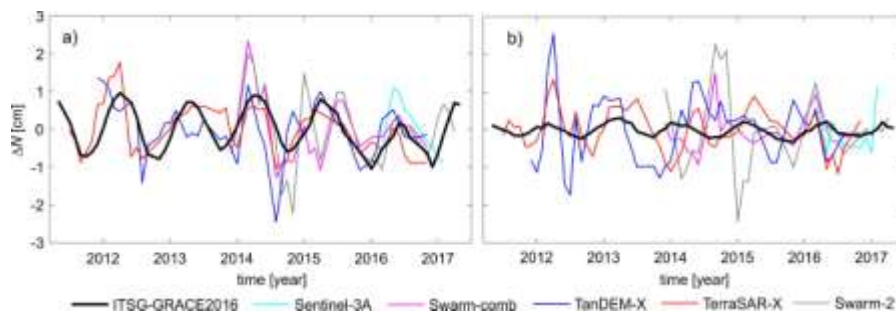


Fig. 30. Smooth time series of geoid height changes obtained from GGMs developed on the basis of data from NDGSM and time series of geoid height changes obtained from GGMs ITSG-GRACE2016 for (a) Amazon basin and (b) Poland

Physical height changes in two study areas: Poland and Turkey, were estimated as a sum of temporal variations of geoid/quasigeoid heights and vertical displacements of the Earth surface using the RL05 GRACE-based GGMs and GRACE-based

global mass concentration (mascon) products as well as load Love numbers from the Preliminary Reference Earth Model (PREM) as input data, and the standard spherical harmonic synthesis, the Green function and the Terzaghi's Principle

method. They were analysed and modelled using two methods: the Seasonal Decomposition (SD) method and the Principal Component Analysis/Empirical Orthogonal Function (PCA/EOF) method (Godah et al., 2018b).

Research on the compliance in gravity changes observed by satellite method with those determined with absolute gravity measurements was also conducted at WUT (Szabo and Barlik, 2018).

Long-term absolute gravimeter observations were compared with GRACE-derived and global hydrology models (Kuczynska-Siehien et al., 2018b).

According to the EU Water Framework Directive every country is obliged to monitor the groundwater level, which is essential for the country's water management. The groundwater consists of water entering the system via pores in the Earth surface. Water is permanently added into system because of the precipitation, leaving because of the evapotranspiration, all the parameters can be acquired exactly from the Global Land Data Assimilation System (GLDAS). Accounting water entering, leaving and stored in the system is called a water budget (balance), which was analysed (Birylo et al., 2018). It was concluded that the greatest influence on the final water budget value has the precipitation (up to $6 \cdot 10^{-5}$ kg/m²/s). The annual amplitude of water budget is about 0; maxima are in February (about $2 \cdot 10^{-5}$ kg/m²/s, in August values of water budget are about 0; minima in April, about $-4 \cdot 10^{-5}$ kg/m²/s, from 2013 $-3 \cdot 10^{-5}$ kg/m²/s.

A variability of the atmospheric energy balance and its impact on the surface fluxes observations using GLDAS was investigated. The Modern-Era Retrospective analysis for Research and Applications version 2 (MERRA-2), Standardized Precipitation Evapotranspiration Index (SPEI) was presented (Birylo, 2018). The calculated atmospheric energy balance values are then compared to the total water storage using GRACE data. In Poland in summer, winter and spring values above normal (values over zero) were observed. During autumn, the atmospheric energy balance is normal (values about zero). Elements of the atmospheric energy balance are only a small part of the total water storage, which was confirmed by comparison with the model from GRACE observations. No linear correlation between the total water storage and the atmospheric balance was noticed.

Nature and climate has been affected by increasing human activity nowadays, so various natural phenomena occurring in different areas should be monitored. GRACE data are appropriate for monitoring the total water storage. The analyses have shown the amplitude of the annual changes of Terrestrial Water Storage (TWS) values at the level of 4 cm, while the monotonic trends computed are so small that the total terrestrial water storage can

be considered stable during the period studied (Rzepecka, 2018).

A geophysical interpretation of polar motion based on the GRACE data and hydrological models was investigated by the team of the Space Research Centre (SRC) of the Polish Academy of Sciences (PAS).

An extensive analysis of the hydrological signals in polar motion excitation using a variety of data sets was conducted. Detailed comparative analysis confirmed earlier conclusion that GRACE observations are more significantly correlated with the observed hydrological excitation than hydrological and climatic models (Nastula et al., 2019). Differences among excitation functions computed using various hydrological models remain considerable. In contrast, gravimetric-hydrological excitation functions determined from GRACE data are internally consistent.

Hydrological excitation of polar motion was investigated using global and regional estimates of TWS computed on the basis of different GLDAS land hydrology models (NOAH, MOSAIC, VIC, CLM) and GRACE data (Sliwinska et al., 2019). The hydrological excitation functions estimated from models were compared with those based on GRACE data and with the geodetic residuals (GAO). In the seasonal spectral band most of the models provide similar amplitude and phase agreement with GRACE and GAO estimations (Fig. 31). However, the GLDAS NOAH of non-seasonal HAM change is closer to GRACE and GAO than any other GLDAS model. A dominant role of soil moisture contribution to the HAM function was observed.

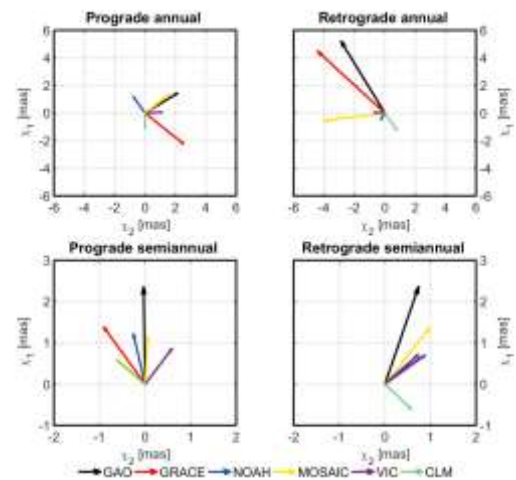


Fig. 31. Phasor diagrams of prograde and retrograde seasonal (annual and semiannual) variation in $\chi_1 + i\chi_2$ for GAO and HAM functions calculated from GRACE data (mean of CSR, JPL and GFZ solution) and GLDAS (NOAH, MOSAIC, VIC and CLM) models; the reference epoch is 2003.0

9. Activities in Satellite Laser Ranging and their use

In 2018 the SLR station BORL at Borowiec of the SRC of PAS tracked 53 different objects, satellites and space debris (cooperative and uncooperative targets), with a total of 1857 full passes (Fig. 38 and Fig. 39). 43 objects were satellites, 29 were Low Earth Orbit (LEO) and 14 were Medium Earth Orbit (MEO) objects. The average RMS ranged from 1.40 cm to 5.17 cm (1374 passes and 21058 normal points). All results were sent to the Crustal Dynamics Data Information System (CDDIS NASA) and Eurolas Data Center (EDC) databanks. The other 10 objects were typical space debris, inactive (defunct) satellites and rocket bodies from the LEO regime. Space debris targets were observed in the framework of Space Debris Study Group (SDSG) of the ILRS. A total of 483 space debris passes were performed with the average RMS ranging from 2.45 cm to 44.83 cm (6085 normal points). All results were sent to the SDSG data bank. The laser ranging measurements of BORL 7811 station support global research in satellite and space debris rotation (tumbling) determination, which are essential for improvement of the theory of the motion of artificial satellites. The first results of the laser tracking of space debris carried out by the BORL station were published (Lejba et al., 2018).

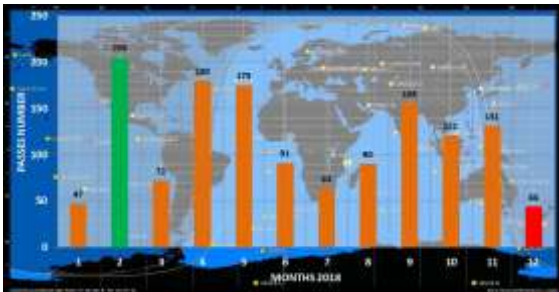


Fig. 38. Observational statistics of satellites for the BORL station in 2018 (green column – the highest number of passes; red column – the lowest number of passes)

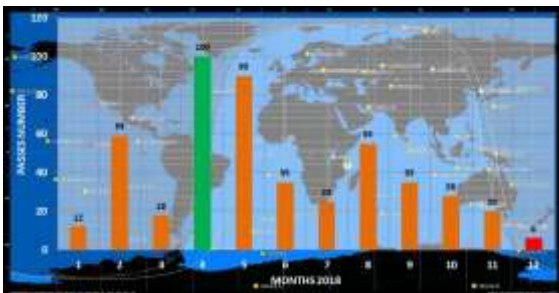


Fig. 39. Observational statistics of space debris for the BORL station in 2018 (green column – the highest number of passes; red column – the lowest number of passes)

9 of tracked satellites were typical passive geodetic-geodynamic satellites (Ajisai, Etalon-1,

Etalon-2, LAGEOS-1, LAGEOS-2, LARETS, LARES, STARLETTE and Stella) which gave in total 589 passes and 6135 normal points. In Table 2 the short observational statistics of these satellites is presented.

Table 2. Observational statistics of geodetic satellites

Sat. name	Passes	Returns	Normal points	Avg RMS [cm]
Ajisai	84	125257	1174	3.71
Etalon-1	3	340	13	3.84
Etalon-2	4	561	19	3.69
LAGEOS-1	116	129404	1084	1.69
LAGEOS-2	91	85247	1083	1.72
LARETS	84	24299	574	2.06
LARES	116	50677	1317	1.48
Stella	29	18261	258	1.97
STARLETTE	62	44753	613	2.03

The largest number of passes was gained for LAGEOS-1 and LARES, the largest number of returns was obtained for LAGEOS-1 and the largest number of normal points is for LARES. The mean RMS ranges from 1.48 cm for LARES (116 passes, 1317 normal points) to 3.84 cm for Etalon-1 (3 passes, 13 normal points).

In 2018, a second independent optical-laser system, dedicated to the Space Surveillance and Tracking (SST) programme, developed by European Space Agency (ESA) and European Commission (EC) was operating at Borowiec. The new system is based on an azimuth-elevation mount with a 65 cm Cassegrain telescope equipped with servo drives. It provides a very fast tracking, with accuracy better than 1 arcsec and a RC 8'' guiding telescope equipped with two fast dedicated optical CMOS cameras. The whole system is controlled by multiplatform steering/tracking software supporting space debris/satellite prediction, real-time laser observations, system calibration, ADSB monitoring, data post-processing and other functions. When fully implemented, the system will operate 24 hours a day, 7 days a week.

Currently, the second setup is able to track, in optical mode, satellites from LEO to GEO regimes. Optical measurements will be used to characterise space missions and SST activity. In the test phase, a special spectroscopic module was dedicated to recording the physical characteristics of tracked targets. The first results of these tests (for the Jason-3 satellite) were presented (Suchodolski et al. 2018). The next step in the development of the new BORL setup, planned for 2019, is the integration of the whole system with a laser module.

10. Geodynamics

IGiK, WAT and WUELS, integrated into the GGOS-PL network, together with the Institute of Geophysics of the Polish Academy of Sciences and with some other institutions continued a common geodynamics research in the framework of the

EPOS-PL project – the Polish Earth science infrastructure integrated with the European Plate Observing System Programme (EPOS) programme.

Activities on developing centres of research infrastructure for geomagnetic and gravimetric data integrated with GNSS infrastructure are continued. In particular, an advanced research is conducted on building-up the Centre of Research Infrastructure for Gravimetric Data (Krynski et al., 2018). A MATLAB package IGIK-TVGMF for computing and analysing temporal variations of gravity/mass functionals from GRACE satellite based global geopotential models for that Centre was developed (Godah, 2018, 2019).

The Multidisciplinary Upper Silesian Episode has been considered as a new holistic approach in building research infrastructure (Olszewska et al., 2018). The Upper Silesian Geophysical Observation System - a unit of EPOS is under development (Mutke et al., 2018). Monitoring of Earth surface displacements using integrated multi-GNSS, gravity, seismic, and InSAR data in test areas (Sosnica et al., 2018c) was initiated.

The geophysical characteristics of the lower lithosphere and asthenosphere in the marginal zone of the East European Craton was investigated in cooperation between the Institute of Geophysics of the University of Warsaw and IGIK (Grad et al., 2018). Gravity records at BG from LCR spring gravimeters and from the iGrav-027 superconducting gravimeter provide a valuable information on low-period seismic surface waves which can be used to determine the Earth's mantle structure (Wilde-Piorko et al., 2018).

De-correlation filters performance for estimating temporal mass variations determined from GRACE-based GGMs over Konya basin were analysed within a common research of IGIK and Selçuk University, Konya, Turkey (Öztürk et al., 2018a, 2018b). The results show that DDK1 and DDK2 filters are most suitable to reduce the noise contained in RL05 GRACE-based GGMs and more effective at revealing mass variations in the study area. They also demonstrate the higher potential of RL05 GRACE-based GGMs developed by GFZ centre to estimate temporal mass variations, than other GGM time series analyzed.

Gravity gradients were forward continued from the orbital altitude of 255 km to the depth of the Mohorovičić discontinuity (Moho) for Central Europe. Components of the Eötvös tensor were obtained from $0.2^\circ \times 0.2^\circ$ grid provided by “Heterogeneous gravity data combination for Earth interior and geophysical exploration research” project “GOCE+”. The results obtained show that forward modelling may be used for recognizing geological structures or mapping in previously undiscovered areas (Lenczuk et al., 2019).

Time series analysis aimed at reliable determination of either velocity or its uncertainty is

an inseparable part of kinematic modelling of the Earth's dynamics. The incorrect interpretation of station coordinate time series may provide the misinterpretation of the geophysical processes in the Earth's interior. Klos et al. (2018a) focused on the estimates of noise character basing on time series of DORIS stations positions. The authors divided the time span that the DORIS stations have been operating within into three different periods. For each of them, they estimated the character of noise. It was noted, that this character changed thorough years from autoregressive process into pure power-law noise, with the quality of data significantly improved. Finally, the velocities of the permanent DORIS stations were provided. The reliable determination of seasonal changes implies the reliability of the determined velocities. Klos et al. (2019) introduced into geodetic community, a methodology named as the Adaptive Wiener Filter (AWF) to estimate time-varying seasonal signals including the character of the original time series. For the synthetic series, AWF has been confronted with the commonly employed Kalman Filter, Singular Spectrum Analysis, Wavelet Decomposition and Least-Squares methods, demonstrating that it provides the accurate estimates for time-varying seasonalities, leaving the noise character intact. In this way, no artificial impact on the velocity estimates is noted. Gruszczynska et al. (2018) proposed the Singular Spectrum Analysis (SSA) as well as its multivariate variant (MSSA) to be an optimum method for description of this variability, but with non-significant influence to the stochastic part as previously applied methods, e.g. wavelet decomposition, Chebyshev polynomials, or Kalman filtering – numerical experiments presented in details in Klos et al. (2018b). Klos et al. (2018c) proposed a two-stage method of subtraction of environmental (atmosphere, non-tidal part of ocean changes and continental hydrosphere) loadings. They proved, that previous attempts failed by changing the stochastic part significantly along with uncertainties of the permanent station velocity. Application of the Improved Singular Spectrum Analysis (ISSA) solved this problem, which was demonstrated on the height changes of 376 permanent IGS stations, derived as the official contribution to ITRF2014. Klos et al. (2018d) provided a General Dilution of Precision (GDP) estimates being the ratio of two uncertainties of velocities. Both uncertainties are determined from two different deterministic models while accounting for stochastic noise at the same time. The authors proved that adding more and more seasonal terms to the series increases the bias of the velocity uncertainties. They estimated that 9 and 17 years of continuous daily observations is needed for flicker and random-walk noise, respectively, to get the GDP decrease below 5%. Gruszczynski et al.

(2018) applied the probabilistic Principal Component Analysis (pPCA). It is a method which allow the spatio-temporal filtering aimed at estimation and subtraction of Common Mode Error (CME) in regional GNSS networks, but with no interpolation of the missing values. The efficiency of the proposed algorithm was firstly tested on the simulated incomplete time series, then CME was estimated for a set of 25 permanent stations from Central Europe. They found, that more than 36% of the total variance represented by time series residuals can be explained by the 1st Principal Component (PC). Since the other PCs variances turned out to be less than 8%, they concluded that that common signals stored in the 1st PC are significant in GNSS residuals.

Acknowledgements

The following researchers submitted data used to elaborate this report: Andrzej Araszkievicz, Monika Birylo, Janusz Bogusz, Grzegorz Bury, Mateusz Drozdzewski, Przemysław Dykowski, Walyeldeen Godah, Kamil Kazmierski, Jan Krynski, Paweł Lejba, Tomasz Liwosz, Adam Lyszkowicz, Tomasz Olszak, Jerzy Rogowski, Witold Rohm, Jarosław Somla, Krzysztof Sosnica, Katarzyna Stepniak, Dariusz Strugarek, Paweł Wielgosz, Radosław Zajdel.

References

- Astafyeva E., Zakharenkova I., Förster M., (2015): *Ionospheric response to the 2015 St. Patrick's Day storm: A global multi-instrumental overview*, J Geophys Res Space Physics 120, pp. 9023–9037, doi:10.1002/2015JA021629
- Barlik M., Olszak T., Pachuta A., Walo J., Prochniewicz D., Szpunar R., Pieniak M., (2018): *Gravity changes at Polish fundamental gravity control network*, GGHS2018 "Gravity, Geoid and Height Systems 2" Symposium, 2nd joint meeting of the International Gravity Field Service and Commission 2 of the IAG, 17–21 September 2018, Copenhagen, Denmark..
- Birylo M., (2018): *Evaluation of the water cycle determined with atmospheric energy balance for the purpose of surface fluxes monitoring*, Proc. 3rd International Conference on Smart and Sustainable Technologies Splitech, Split, Croatia, 26–29 June 2018.
- Birylo M., Rzepecka Z., Nastula J., (2018): *Assessment of the water budget from GLDAS model*, Proc. Baltic Geodetic Congress (BGC Geomatics) 2018, 21–23 June 2018, Olsztyn, Poland.
- Bury G., Sosnica K., Zajdel R. (2017): *How many SLR observations and how many stations are needed for deriving high-quality multi-GNSS orbits?*, Proceedings from the ILRS Technical Workshop "Improving ILRS Performance to Meet Future GGOS Requirements", Riga, Latvia, 02–05 October 2017, https://cdsis.nasa.gov/2017_Technical_Workshop/docs/papers/session1/ilrsTW2017_s1_paper_Bury.pdf
- Bury G., Sosnica K., Zajdel R., (2019): *Impact of the Atmospheric Non-tidal Pressure Loading on Global Geodetic Parameters Based on Satellite Laser Ranging to GNSS*, IEEE Transactions on Geoscience and Remote Sensing, DOI: 10.1109/TGRS.2018.2885845
- Drozdzewski M., Sosnica K., (2018): *Satellite laser ranging as a tool for the recovery of tropospheric gradients*, Atmospheric Research, 212, pp. 33–42, DOI: 10.1016/j.atmosres.2018.04.028
- Dykowski P., Krynski J., Sekowski M., (2018a): *The use of the A10-020 absolute gravimeter for the establishment and modernization of national gravity controls in Europe*, Geophysical Research Abstracts, Vol. 20, EGU2018-2025, EGU General Assembly 2018, 8–13 April, Vienna, Austria.
- Dykowski P., Sekowski M., Krynski J., Wilde-Piorko M., (2018b): *Report on the Borowa Gora (BG) IGETS Station*, 1st Workshop on the International Geodynamics and Earth Tide Service (IGESTS), 18–20 June 2018, Potsdam, Germany.
- Dykowski P., Krynski J., Wilde-Piorko M., Sekowski M., (2018c): *Assessment of iGrav-027 superconducting gravimeter for validation of gravity variations based on atmospheric and hydrological models*, GGHS2018 "Gravity, Geoid and Height Systems 2" Symposium, 2nd joint meeting of the International Gravity Field Service and Commission 2 of the IAG, 17–21 September 2018, Copenhagen, Denmark.
- Engfeldt A., Lidberg M., Sekowski M., Dykowski P., Krynski J., Ågren J., Olsson P.-A., Bryskhe H., Steffen H., Nielsen J.E., (2018a): *RG 2000 – the new gravity system of Sweden*, Symposium of the IAG Subcommission for Europe (EUREF) held in Amsterdam, the Netherlands, 30 May – 1 June 2018 <http://www.euref.eu/symposia/2018Amsterdam/03-09-Lidberg.pdf>
- Engfeldt A., Lidberg M., Sekowski M., Dykowski P., Krynski J., Ågren J., Olsson P.-A., Bryskhe H., Steffen H., Nielsen J.E., (2018b): *RG 2000 – the new gravity reference frame of Sweden*, FIG Congress 2018, 6–11 May 2018, Istanbul, Turkey.
- Godah W., (2018a): *IGiK-TVGMF: A Matlab® GUIs package for computing, analysing and modelling temporal variations of gravity/mass functionals from GRACE satellite based global geopotential models*, GRACE Scientific Team Meeting, 9–11 October 2018, Potsdam, Germany. https://presentations.copernicus.org/GSTM-2018-6_presentation.pdf
- Godah W., (2018b): *On the determination, analysis and modelling of temporal variations of gravity/mass functionals from GRACE/GRACE-FO satellite missions*, The 1st Scientific and Technical Conference dedicated to the EPOS-PL project, 19–21 November 2018, Warsaw, Poland.
- Godah W., (2019): *IGiK-TVGMF: A MATLAB package for computing and analysing temporal variations of gravity/mass functionals from GRACE satellite based global geopotential models*, Computers & Geosciences, Vol. 123, pp. 47–58. <https://doi.org/10.1016/j.cageo.2018.11.008>
- Godah W., Krynski J., Szelachowska M., (2018a): *The use of absolute gravity data for the validation of Global Geopotential Models and for improving quasigeoid heights determined from satellite-only Global Geopotential Models*, Journal of Applied Geophysics, Vol. 152, May 2018, pp. 38–47, doi:10.1016/j.jappgeo.2018.03.002.
- Godah W., Szelachowska M., Öztürk E.Z., Krynski J., (2018b): *On the contribution of physical height changes estimated with the use of GRACE satellite mission data to the modernization of a national vertical system*, AGU Fall Meeting, 10–14 December 2018, Washington, D.C., USA.

- Godah W., Szelachowska M., Krynski J., (2018c): *On the determination of temporal variations of geoid heights from GGMs based on SST-hl data of non-dedicated gravity satellite missions*, GRACE Science Team Meeting, 9–11 October 2018, Potsdam, Germany.
- Godah W., Szelachowska M., Krynski J., (2019): *On the recovery of temporal variations of geoid heights determined with the use of GGMs based on SST-hl data from non-dedicated gravity satellite missions*, The Bulletin of Geodetic Sciences (ISSN: 1982-2170).
- Grad M., Puziewicz J., Majorowicz J., Chrapkiewicz K., Lepore S., Polkowski M., Wilde-Piorko M., (2018): *The geophysical characteristic of the lower lithosphere and asthenosphere in the marginal zone of the East European Craton*, International Journal of Earth Sciences, (Geol Rundsch) Vol. 107, Issue 8, pp 2711–2726, doi.org/10.1007/s00531-018-1621-y
- Gruszczynska M., Rosat S., Klos A., Gruszczynski M., Bogusz J., (2018): *Multichannel Singular Spectrum Analysis in the estimates of common environmental effects affecting GPS observations*, Pure and Applied Geophysics, 175(2018), pp. 1805–1822, doi:10.1007/s00024-018-1814-0
- Gruszczynski M., Klos A., Bogusz J., (2018): *A filtering of incomplete GNSS position time series with probabilistic Principal Component Analysis*, Pure and Applied Geophysics, 175(2018), pp. 1841–1867, doi: 10.1007/s00024-018-1856-3
- Hordyniec P., (2018): *Simulation of liquid water and ice contributions to bending angle profiles in the radio occultation technique*, Advances in Space Research, 62(5), pp. 1075–1089, doi: 10.1016/j.asr.2018.06.026
- Hordyniec P., Kaplon J., Rohm W., Kryza M., (2018a): *Residuals of tropospheric delays from GNSS data and ray-tracing as a potential indicator of rain and clouds*, Remote Sensing, 10(12), 1917, pp. 1–26, doi: 10.3390/rs10121917
- Hordyniec P., Huang C.-Y., Liu C.-Y., Rohm W., Chen S.-Y., (2018b): *GNSS radio occultation profiles in the neutral atmosphere from inversion of excess phase data*, Terrestrial, Atmospheric and Oceanic Sciences. doi: 10.3319/TAO.2018.10.12.01
- Jarmolowski W., Ren X., Wielgosz P., Krypiak-Gregorczyk A., (2019): *On the advantage of stochastic methods in the modeling of ionospheric total electron content: Southeast Asia case study*, Measurement Science and Technology, 30(4), https://dx.doi.org/10.1088/1361-6501/ab0268
- Kazmierski K., (2018): *Performance of Absolute Real-Time Multi-GNSS Kinematic Positioning*, Artificial Satellites, 53(2), pp. 75–88, doi: 10.2478/arsa-2018-0007
- Kazmierski K., Hadas T., Sosnica K., (2018a): *Weighting of Multi-GNSS Observations in Real-Time Precise Point Positioning*, Remote Sensing 10(1), 84, doi: 10.3390/rs10010084
- Kazmierski K., Sosnica K., Hadas T., (2018b): *Quality assessment of multi-GNSS orbits and clocks for real-time Precise Point Positioning*, GPS Solutions, Vol. online No 22:11, Berlin – Heidelberg 2018, pp. 1–12, DOI: 10.1007/s10291-017-0678-6
- Klos A., Bogusz J., Moreaux G., (2018a): *Stochastic models in the DORIS position time series: estimates for IDS contribution to ITRF2014*, Journal of Geodesy, 92:743–763, doi: 10.1007/s00190-017-1092-0
- Klos A., Bos M.S., Bogusz J., (2018b): *Detecting time-varying seasonal signal in GPS position time series with different noise levels*, GPS Solutions, Vol. 22, Issue 1, DOI:10.1007/s10291-017-0686-6
- Klos A., Gruszczynska M., Bos M.S., Boy J.-P., Bogusz J., (2018c): *Estimates of vertical velocity errors for IGS ITRF2014 stations by applying the Improved Singular Spectrum Analysis method and environmental loading models*, Pure and Applied Geophysics, 175(2018), pp. 1823–1840, doi:10.1007/s00024-017-1494-1
- Klos A., Olivares G., Teferle F.N., Hunegnaw A., Bogusz J., (2018d): *On the combined effect of periodic signals and colored noise on velocity uncertainties*, GPS Solutions, 22:1, doi: 10.1007/s10291-017-0674-x
- Klos A., Bos M.S., Fernandes R.M.S., Bogusz J., (2019): *Noise-Dependent Adaptation of the Wiener Filter for the GPS position time series*, Mathematical Geosciences, doi: 10.1007/s11004-018-9760-z
- Krynski J., Rogowski J.B., (2018): *National Report of Poland to EUREF 2018*, Symposium of the IAG Subcommission for Europe (EUREF) held in Amsterdam, the Netherlands, 30 May – 1 June 2018 <http://euref.eu/symposia/2018Amsterdam/05-18-p-Poland.pdf>
- Krynski J., Wilde-Piorko M., Dykowski P., Sekowski M., Godah W., Szelachowska M., (2018): *Building-up the Centre of Research Infrastructure for Gravimetric Data (CIBOG)* (in Polish), 1 konferencja naukowo-techniczna poświęcona projektowi EPOS-PL, Jachranka, 19–21 November 2018.
- Krynski J., Rogowski J.B., Liwosz T., (2019a): *Research on reference frames and reference networks in Poland in 2015-2018*, Geodesy and Cartography, Vol. 68, No 1, 2019, DOI: 10.24425/gac.2019.126093
- Krynski J., Dykowski P., Olszak T., (2019b): *Research on gravity field modelling and gravimetry in Poland in 2015-2018*, Geodesy and Cartography, Vol. 68, No 1, 2019, DOI: 10.24425/gac.2019.126094
- Krypiak-Gregorczyk A., (2018): *Ionosphere response to three extreme events occurring near spring equinox in 2012, 2013 and 2015, observed by regional GNSS-TEC model*, Journal of Geodesy, doi.org/10.1007/s00190-018-1216-1
- Krypiak-Gregorczyk A., Wielgosz P., Borkowski A., (2017): *Ionosphere model for European region based on multi-GNSS data and TPS interpolation*, Remote Sens. 9:1221. <https://doi.org/10.3390/rs9121221>
- Krypiak-Gregorczyk A., Wielgosz P., (2018): *Carrier phase bias estimation of geometry-free linear combination of GNSS signals for ionospheric TEC modeling*, GPS Solutions, Vol. 22, No 2, pp. 1–9. doi:10.1007/s10291-018-0711-4
- Kuczynska-Siehien J., Lyszkowicz A., Sideris M.G., (2018a): *Evaluation of Altimetry Data in the Baltic Sea Region for Computation of New Quasigeoid Models over Poland*, In: IAG Symposia, Springer, Berlin, Heidelberg, pp. 1–10, DOI https://doi.org/10.1007/1345_2018_35
- Kuczynska-Siehien J., Piretzidis D., Sideris M., Olszak T., Szabó V., (2018b): *Comparison of long-term absolute gravimeter observations with GRACE and global hydrology models*, GGHS2018 “Gravity, Geoid and Height Systems 2” Symposium, 2nd joint meeting of the International Gravity Field Service and Commission 2 of the IAG, 17–21 September 2018, Copenhagen, Denmark.
- Lasota E., Rohm W., Liu C.-Y., Hordyniec P., (2018): *Cloud Detection from Radio Occultation Measurements in Tropical Cyclones*, Atmosphere 2018, 9, 418.
- Lejba P., Suchodolski T., Michalek P., Bartoszak J., Zapasnik S., Schillak S., (2018): *First laser measurements to space debris in Poland*, Advances in Space Research, Vol. 61, Issue 10, pp. 2609–2616, DOI: <https://doi.org/10.1016/j.asr.2018.02.033>
- Lenczuk A., Bogusz J., Olszak T., Barlik M., (2019): *Studying the sensitivity of GOCE gravity gradients to the crustal structure: case study of Central Europe*, Acta Geodaetica et Geophysica. Vol. Published online 05.02.2019, pp. 1–16, doi 10.1007/s40328-019-00250-y

- Liwosz, T., Araszkiewicz A., (2018): *EPN Analysis Coordinator Report*, Symposium of the IAG Subcommission for Europe (EUREF) held in Amsterdam, Netherlands, 31 May – 2 June 2018, <http://www.euref.eu/symposia/2018Amsterdam/02-02-Liwosz.pdf>
- Lyszkowicz A., Bernatowicz A., (2018a): *Geocentric changes of the mean sea level of the Baltic Sea from altimeter and tide gauge data*, IEEE Transaction, DOI: 10.1109/BGC-Geomatics.2018.00044
- Lyszkowicz A., Bernatowicz A., (2018b): *Geocentric sea level changes at tide gauge station in Władysławowo*, FIG 2018 Proceedings, ISBN 978-87-92853-78-3
- Mota G.V., Shuli S., Stepniak K., (2018): *Assessment of integrated water vapor through ground-based GNSS dataset over central and northeastern Amazonia*, AGU Fall Meeting, Washington, USA, 10–14 December 2018.
- Mutke G., Kotyrba A., Lurka A., Olszewska D., Dykowski P., Borkowski A., Araszkiewicz A., Baranski A. (2018): *Upper Silesian Geophysical Observation System - a unit of European Plate Observing System*, 4th International Conference on APPLIED GEOPHYSICS 2018, 28–29 June 2018, Krakow, Poland.
- Nastula J., Winska M., Sliwinska J., Salstein D., (2019): *Hydrological signals in polar motion excitation – Evidence after fifteen years of the GRACE mission*, Journal of Geodynamics, 124(2018), pp. 119–132. <https://doi.org/10.1016/j.jog.2019.01.014>
- Nykiel G., Zanimonskiy Y., Koloskov A., Figurski M., (2018): *Estimation of the height of ionospheric inhomogeneities based on TEC variations maps obtained from GPS observations*, 42nd COSPAR Scientific Assembly 2018 URL: https://www.cospas-assembly.org/uploads/documents/AbstractCD_COSPAR-18.iso
- Olszak T., Marjanska D., Pietka D., (2018): *Validation and fitting of European Gravimetric Geoid EGG08 in context of realisation of EVRS system in Poland*, GGHS2018 “Gravity, Geoid and Height Systems 2” Symposium, 2nd joint meeting of the International Gravity Field Service and Commission 2 of the IAG, 17–21 September 2018, Copenhagen, Denmark.
- Olszewska D., Lizurek G., Mutke G., Krynski J., Rohm W., Araszkiewicz A., Baranski A., (2018): *Multidisciplinary Upper Silesian Episode as a new holistic approach in building research infrastructure*, The 36th General Assembly of the European Seismological Commission, 2–7 September 2018, Valletta, Malta.
- Öztürk E.Z., Godah W., Abbak R.A., (2018a): *Evaluation of RL05 GRACE Based Global Geopotential Models on a Regional Scale: A case study of Turkey*, EGU General Assembly 2018, Vienna, Austria, 8–13 April 2018, Geophysical Research Abstracts, Vol. 20, EGU2018-2141. <https://meetingorganizer.copernicus.org/EGU2018/EGU2018-2141.pdf>
- Öztürk E.Z., Godah W., Abbak R.A., (2018b): *Analysis of De-correlation filters performance for estimating temporal mass variations determined from GRACE-based GGMS over Konya basin*, FIG Congress 2018, 6–11 May 2018, Istanbul, Turkey.
- Rzepecka Z., (2018): *Analysis of TWS variations on the terrain of the Vistula and Odra basins in Poland*, Proc. 5th International Conference on Time Series and Forecasting, 19-21 September 2018, Granada, Spain.
- Sliwinska J., Winska M., Nastula J., (2019): *Terrestrial water storage variations and their effect on polar motion*, Acta Geophysica, 67(1), pp. 17–39, <https://doi.org/10.1007/s11600-018-0227-x>
- Sosnica K., Prange L., Kazmierski K., Bury G., Drozdowski M., Zajdel R., Hadaś T., (2018a): *Validation of Galileo orbits using SLR with a focus on satellites launched into incorrect orbital planes*, Journal of Geodesy 89(2), pp. 131–148, DOI: 10.1007/s00190-017-1050-x
- Sosnica K., Bury G., Zajdel R., (2018b): *Contribution of multi-GNSS constellation to SLR-derived terrestrial reference frame*, Geophysical Research Letters 45(5), pp. 2339–2348, DOI: 10.1002/2017GL076850
- Sosnica K., Kaplon J., Rohm W., Kudlacik I., Zajdel R., Hadaś T., Bosy J., Sierny J., Borkowski A., Krynski J., Dykowski P., Mutke G., Kotyrba A., Olszewska D., (2018c): *Monitoring of Earth surface displacements using integrated multi-GNSS, gravity, seismic, and InSAR data in the framework of GGOS-PL++*, 42nd COSPAR Scientific Assembly, Pasadena, California, 14–22 July 2018.
- Stepniak K., Bock O., Bosser P., (2018): *Comparison of tropospheric estimates from DD and PPP processing approaches for climate monitoring*, EGU General Assembly 2018, Vienna, Austria, 8–13 April 2018.
- Suchodolski T., Lejba P., Michalek P., Bartoszak J., Zapaśnik S., (2018): *Mission characterization of LEO targets*, 21st International Workshop on Laser Ranging (International Workshop on Space Debris Management and Mitigation), Canberra, Australia, 5–9 November.
- Szabo V., Barlik M., (2018): *Analysis of changes compliance in gravity observed by satellite method with absolute measurements*, Geophysical Research Abstracts, Vol. 20, EGU2018-9315, 2018, EGU General Assembly 2018.
- Wilde-Piorko M., Dykowski P., Polkowski M., Sekowski M., Grad M., Krynski J., (2018): *Determination of the Earth’s mantle structure from low-period seismic surface waves recorded by superconducting and spring gravimeters at the Borowa Góra Gora Observatory*, 1st Workshop on the International Geodynamics and Earth Tide Service (IGESTS), 18–20 June 2018, Potsdam, Germany.
- Winska M., Sliwinska J., (2019): *Assessing hydrological signal in polar motion from observations and geophysical models*, Studia Geophysica et Geodaetica, 63(2019), pp. 95–117, <https://doi.org/10.1007/s11200-018-1028-z>
- Zajdel R., Sosnica K., Bury G., (2017): *A New Online Service for the Validation of Multi-GNSS Orbits Using SLR*, Remote Sensing, Vol. 9(10) 1049, pp. 1–22, DOI: 10.3390/rs9101049
- Zajdel R., Sosnica K., Bury G., Kazmierski K., (2018): *GOVUS: A new on-line service for Galileo, GLONASS, BeiDou and QZSS orbit validation using Satellite Laser Ranging*, ESA Scientific and Technical Reports, No 2(3), Valencia, Spain.